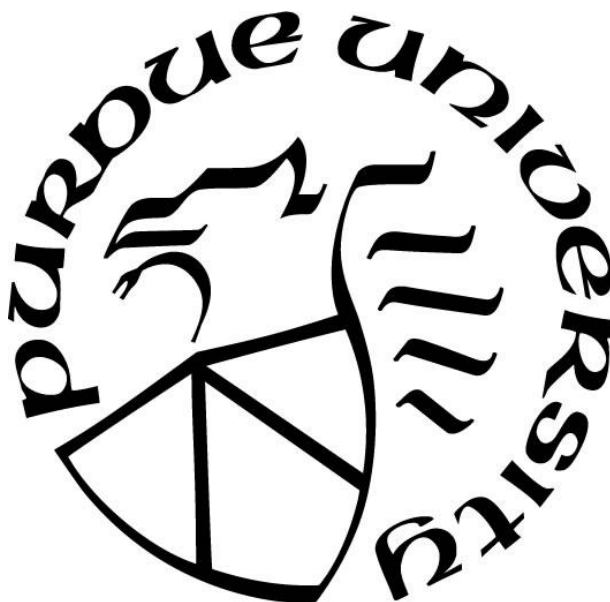# DEVELOPMENT OF NOVEL LIQUID CHROMATOGRAPHY STATIONARY PHASES FOR IMPROVED CHARACTERIZATION OF BIOPHARMACEUTICALS

by

Cameron Schwartz

A Dissertation

Submitted to the Faculty of Purdue University

In Partial Fulfillment of the Requirements for the degree of

Doctor of Philosophy

Department of Chemistry

West Lafayette, Indiana

August 2021

THE PURDUE UNIVERSITY GRADUATE SCHOOL
STATEMENT OF COMMITTEE APPROVAL

Dr. Mary J Wirth

Department of Chemisry

Dr. Hilkka L Kenttämaa .

Department of Chemistry

Dr. Corey Thompson

Department of Chemistry

Dr. Jesse Zhang

Department of Chemistry

Approved by:

Dr. Christine Hrycyna

ACKNOWLEDGMENTS

I would just like to say thank you to my parents, grandparents, and friends that have been supportive and helped along the way.

TABLE OF CONTENTS

LIST OF TABLES

LIST OF FIGURES

ABSTRACT

Monoclonal antibodies are large, complex biomolecules that can be difficult to characterize. Characterization is important because of the various post translational modifications that can occur during manufacturing, processing, and storage. Some modifications can lead to efficacy and safety issues and therefore are heavily monitored. A leading way to monitor various modifications is by using liquid chromatography. The high sensitivity, reproducibility, and ability to quantitate analytes makes it very attractive for monoclonal antibody characterization. The large molecular size of monoclonal antibodies (150 kDa) makes them challenging to separate efficiently and with high enough resolution to be helpful. New column technologies that would help improve protein separation efficiencies and slectivities would greatly help in this challenging process. In this thesis, three novel bonded phases are developed for the separation of monoclonal antibodies including a weak anion and cation exchanger (WAX, CEX) for the separation of charged species as well as a novel hydrophilic interaction chromatography (HILIC) for the separation of glycoforms. Column develop is achieved by optimizing selectivity and improving efficiency of separations by altering particle surface chemistry.

CHAPTER 1.   LIQUID CHROMATOGRAPHY OF MONOCLONAL ANTIBODIES

1.1   Abstract

The large size and inherent heterogeneity of therapeutic monoclonal antibodies (mAbs) make characterization a unique and difficult challenge compared to small-molecule drugs. High performance (HPLC) and ultra-high performance (UHPLC) liquid chromatography are common techniques used to help in characterization of mAbs. This chapter reviews mAb structure and heterogeneity as well as common liquid chromatography techniques used in characterization. Column characteristics like particle morphology are also discussed in terms of large molecule separations.

1.2   Monoclonal Antibodies

Monoclonal antibody (mAbs) drugs have been around for decades, and recently the 100th mAb drug has been approved by the FDA (1). MAbs have been developed to treat numerous diseases, inlcuding cancer (2,3), autoimmune (3), migraines(4), Chrone's disease (5), and many more. What makes mAbs so attractive as a drug class is the concept of using them as a "magic bullet" (6) to specifically interact with a target of interest, leading to increased efficacy and a decrease in side effects caused by interactions with cells not of interest.

MAbs are large (150 kDa), heterogeneous molecules manufactured typically using genetically modified Chinese hamster ovary cells in a bioreactor (7). Monoclonal refers to the identical sequences of the expressed antibodies. The immunoglobulin (Ig) family of mAbs is divided into five isotypes: IgA, IgD, IgE, IgG, and IgM. IgGs are the only ones currently used for therapeutic purposes, and this isotype has 4 subclasses: IgG1, IgG2, IgG3, and IgG4. IgG3 is the only one not used in therapeutics because of relatively short half-life and faster clearance rate from the body compared to the others (21). Figure 1.1 shows a schematic structure of an IgG1, indicating its specific structural parts. MAbs are comprised of two light chains (25 kDa each) and 2 heavy chains (50 kDa each). The structure is commonly described as being a Y shape, with the top part, or arms, being referred to as the Fab (antigen binding fragment), and the bottom part being referred to as the Fc (crystallizable fragment). The Fab is responsible for binding to the

target of interest, whereas the Fc is responsible for inducing an immune response. The ends of the Fab are variable, forming the complementarity determining region. In designing drugs, the amino acid sequence is adjusted to bind to the target of interest. The region at which the Fc and Fab connect is referred to as the hinge region and it is made up of either 2 (IgG1, IgG4) or 4 (IgG2) disulfide bonds.

1.2.1 mAb Modification and LC characterization methods

The complex structure and biological manufacturing of mAbs allow for a variety of modifications to occur, which can be chemical or enzymatic, resulting in protein heterogeneity (8). Many modifications lead to variants that affect the safety and efficacy of the mAb (9-1l). These modifications include deamidation (8,12), isomerization (8), succinimide formation (8,15), incomplete C terminal lysine clipping (14), hydrolysis (15) disulfide shuffling (8), aggregation (8), glycosylation (8,10), oxidation (8,13), N-terminal pyroglutamate formation (8,12), and fragmentation (8), and more. Those modifications that do not have safety or efficacy issues are still required to be characterized to monitor consistency in mAb manufacturing.

Deamidation and isomerization are two such modifications that can impact mAb structure and therefore stability and efficacy. Asn can undergo deamination to yield Asp, isomerization can yield isoAsp or form succinimide (Asu) (14). These have been shown to reduce binding affinities and antibody potency (16.17). These can also induce a conformational change exposing more basic residues. This allows for characterization based on charge using techniques like cation and anion exchange (CEX,AEX) or isoelectric focusing (IEF) (16). Reverse phase and hydrophobic interaction chromatography (HIC) have also been used to characterize isomerization, sometimes providing higher resolution than charge based separations. (18,19)

Oxidation of methionine and tryptophane can also be problematic modifications that occur during mAb purification and storage that can lead to aggregation or stability issues(20). Specifically methionine oxidation in the Fc region at Met 252 or 428 will decrease stability due to inducing a confirmational change (21). Characterization of oxidation variants can be achieved by HIC because of the change in polarity of the native mAb, causing oxidized variants to elute earlier than nonoxidized species.(19) Ion exchange can also be used in separation of oxidized species, with AEX reporting better resolution than CEX (13). The oxidation of methionine

results in a more basic species because of a conformational change and not a change in isoelectric point; therefore, IEF does not work to separate these variants.

MAbs contain an N-glycosylation site at Asp297 in the Fc region, but may additionally contain glycosylation sites in the variable region of the heavy or light chains in the Fab region (22) Only small amounts of non-glycosylated antibodies are observed. Glycosylation helps with mAb stability as well as helping mediate an immune response. Nonhuman glycans can be produced during manufacturing due to the use of a nonhuman cell line, and these can lead to immunogenicity or deadly side effects (23). Glycans are biantennary with various combinations of sugar groups, including N-acetylglucosamine, mannose, galactose, sialic acid, and fucose. The different combinations of sugar group leads to large heterogeneity in glycans after mAb manufacturing. Glycosylation is usually characterized at the glycan level by cleavage of the glycan using N-glycosidase (PNGase F) followed by fluorescence labeling for detection after separation by HILIC (24). They may also be separated using IEC (25) or capillary electrophoresis (26) and can be identified in line using mass spectrometry. The process of cleaving the glycan from the antibody, followed by labeling, is a laborious process taking 14 hours of time. Recent studies have introduced a streamlined, automated workflow using HILIC to separate the glycosylated Fc fragment, which is generated via Ides digestion to cleave the Fc and Fab portions,. (27-30) This also allows for faster glycan analysis and the use of LC-MS/MS for identification and location of glycosylation.

Disulfide bonds are essential to the 3D antibody structure and its integrity (31). Light chains are connected to the heavy chain in the Fab region by one disulfide bond, and the heavy chains are connected to one another in the hinge region through either two (IgG1 and IgG4) or four (IgG2) disulfide bonds. There are other intra-chain disulfide bonds throughout the mAb that help maintain the globular structure and integrity of the mAb (32). All cysteine residues should be connected to one another through disulfide bonds but low levels of sulfhydryl groups have been detected in mAbs indicating this is not always the case (33). Sulfhydryl bonds result from incomplete formation of disulfide bonds or disulfide bond degradation. The presence of sulfhydryl groups, and fewer disulfide bonds, may lead to structural changes in the mAb that reduce stability and efficacy (34). Disulfide bond characterization has been done using reverse phase chromatography (RPLC) (31) as well as capillary electrophoresis (CE) (35)

1.3   Liquid Chromatography of mAbs

Liquid chromatography is a powerful technique used in many different industries including the pharmaceutical industry (36), helping with drug discovery, development and manufacturing (37). HPLC separation of mAbs is a common practice, but can be very challenging because of the large size and numerous interactions that can take place between the analyte and the bonded phase. The increase in size and number of interaction results in a slower mass-transfer for proteins. It is important to consider the differences between small molecule and large molecule protein separations when considering new column development, which will be discussed in later chapters. Figure 1.2 describes the contributions to resolution (Rs) from efficiency (N), selectivity (α), and the retention factor (k). Efficiency and selectivity changes with molecular weight need to be considered when developing new HPLC bonded phases. Understanding the theory is key to improving resolution and therefore will be discussed in the following sections.

1.3.1   Efficiency

Efficiency in chromatography is defined by the total number of theoretical plates, N, which is defined by equation 1.1, where L is the length of the column and H is the theoretical plate height.

$$N = \frac{L}{H} \qquad (1.1)$$

Equation ? shows that resolution is proportional to the square root of N. Therefore, one must quadruple the column length to increase efficiency by a factor of 2. Reducing the theoretical plate height improves efficiency, with N being inversely proportional to plate height. Therefore, if one wants to determine the efficiency independent of column length, H is used to compare efficiencies between bonded phases. The plate height depends on linear velocity, v, as shown by the van Deemter equation (Figure 1.3). Three terms make up the van Deemter equation, the A, B, and C terms which represent the physical, kinetic, and thermodynamic properties of the separation, respectively (38).

The A term represents eddy diffusion, which describes the band broadening from the multiple pathways an analyte can take through a packed column. The A term is independent of mobile phase velocity and only depends on the quality of the packing and particle size.

The B term represents longitudinal diffusion that results from the random displacements over time of analyte molecules . The B term depends on both mobile phase velocity and the diffusion coefficient of the analyte. For large molecules like mAbs, the diffusion coefficient is on the order of 10^{-6}, and since the B term is proportional to the diffusion coefficient, it is negligible in most situations for mAb separations.

The C term describes the resistance to mass transfer and is split into three parts. The C_m term is from the parabolic flow profile that results from wall effects from the mobile phase interacting with the solid particles. This leads to band broadening due to the distributions of mobile phase velocities. The C_p term is from the diffusion of the analyte in and out of porous particles. Pore size is an important factor to consider in mAb separations for this reason. If pore sizes approach the large size of mAbs, this can lead to slower intraparticle diffusion and efficient separations. The C_s term is from the adsorption and desorption kinetics of the analyte with the stationary phase. This contribution is independent of particle morphology and depends only on mobile phase velocity, the bonded phase, and the analyte.

1.3.2   Selectivity

Selectivity, unlike efficiency, does not depend on particle or pore size. It is dependent on the chemical makeup of the bonded phase and the interactions that analytes have with that bonded phase. Selectivity determines the distance between the center of eluting peaks, not the peak widths. The selectivity is defined by α, which is the ratio of retention factors of two analytes of interest, k_2/k_1. The larger the difference in retention factors, the larger α, and the greater the selectivity of the bonded phase for that particular separation. Equation ? shows that resolution is proportional to (1- α). This shows that a larger increase in resolution may be made by finding a more selective bonded phase than by improving efficiency.

1.3.3   Silica particle morphologies

There are three major types of silica particle morphologies used in LC separations. They are shown in figure 1.4 as nonporous particles, fully porous particles, and superficially porous particles. Each provide specific advantages, and disadvantages when it comes to protein separations. Totally porous particles are the most commonly used silica support. They consist of

small particles fused together in a way that produces a larger particle that has pores in between the fused smaller particles, producing a high surface area compared to similarly sized nonporous particles. The average pore size can range from 6 nm all the way up to 30 nm or more. The porous particles allow for a large surface area, but the relatively small size compared to large proteins causes a large C_p term because of the slow diffusion of the protein into and out of the pores (39). This leads to less efficient separations for large molecules compared to small molecules.

Nonporous particles decrease the C_p term by eliminating intraparticle diffusion resulting in improved mass transfer compared to porous particles (40). This comes at a price though of lower surface area. Nonporous particles also pack more homogeneously than porous particles because they generally have a more uniformed size distribution than porous or superficially porous particles. This improves the A term and allows for more efficient separations.

The third particle morphology is superficially porous particles (SPP). SPP have a solid, nonporous core, surrounded by smaller particles fused together to produce a porous shell (41). The nonporous core allows for a decrease in mass-transfer and lower C_p term compared to fully porous particles, although they still have a larger C_p term than nonporous. The porous shell allows for a higher surface area, resulting in larger capacities than nonporous particles. SPP try to combine the advantages of using both nonporous particles and fully porous particles. Unlike fully porous particles, the pore size for SPP can be much larger. SPP have recently been developed with an average pore size of 100 nm, allowing the protein to enter more the of porous structure increasing the surface area of interaction, as well as decreasing the mass transfer term caused by particles with smaller pores. (42-44)

1.4   Column Optimization Considerations for Protein Separations

When developing a new bonded phase for protein separations, efficiency and selectivity need to be considered. The B term for efficiency is negligible because of the large analyte size, and the A term is fairly consistent as long as you have narrow particle size distribution and good packing technique. Therefore, the C term for efficiency as well as selectivity are the two main factors that need to be considered during column development. As we discussed earlier, C_p represents intraparticle diffusion of the analyte into and out of the pores. For large proteins, these pores can lead to slower intraparticle diffusion because of decreased pore volume and lead to less

efficient separations. Large porous particles have been developed to improve upon this C_p term (45). Another strategy is to use nonporous particles which eliminates the C_p term altogether and will result in more efficient separations of large proteins. Using nonporous particles also tends to decrease particles size distribution because it is easy to control the size of nonporous particles during the Stober process than porous particles (46). This does come at the price of increased pressure and a decrease in capacity, but instrumentation today allows for high pressure separations; therefore, pressure is no longer as much as a limitation as it was in the past.

1.5 Reference

[1] Mullard, A. (2021) FDA approves 100th monoclonal antibody produce. Nature Reviews Drug Discovery. doi: https://doi.org/10.1038/d41573-021-00079-7.

[2] A. Scott, J. A. (2012). Monoclonal antibodies in cancer therapy. Cancer Immunity, 12, 14

[3] Hafeez, U., Gan, H. K., & Scott, A. M. (2018, August 1). Monoclonal antibodies as immunomodulatory therapy against cancer and autoimmune diseases. Current Opinion in Pharmacology.

[4] Reuter, U., (2018) A Review of Monoclonal Antibody Therapies and Other Preventive Treatments in Migraine. *Headache.* 58, 48-59.

[5] Drewe, E., Powell, R.J. (2002) Clinically useful monoclonal antibodies in treatment. *Journal of Clinical Pathology*. 55(2), 81-85.

[6] Brodsky, F. M. (1988). Monoclonal Antibodies as Magic Bullets. *Pharmaceutical Research: An Official Journal of the American Association of Pharmaceutical Scientists*.

[7] Li, F., Vijayasankaran, N., Shen, Yijuan., Kiss, R., Amuanullah, A., (2010) Cell culture processes for monoclonal antibody production. *MAbs*. 2(5), 466-477.

[8] Liu, H., Gaza-Bulesco, G., Faldu, D., Chumsae, C., Sun, J. (2008) Heterogeneity of Monoclonal Antibodies. *Journal of Pharmaceutical Sciences*. 97(7) 2426-2447

[9] Hermeling, S., Crommelin, D., Schelleckens, H., Jiskoot, W. (2004) Structure-Immunogenicity Relationships of Therapeutic Proteins. *Pharmaceutical Research* 21(6), 897-903.

[10] Higel, F., Seidl, A., Sörgel, F., & Friess, W. (2016, March 1). N-glycosylation heterogeneity and the influence on structure, function and pharmacokinetics of monoclonal antibodies and Fc fusion proteins. *European Journal of Pharmaceutics and Biopharmaceutics*.

[11] Xu, Y., Wang, D., Mason, B., Rossomando, T., Li, N., Liu, D., Cheung, J., Xu, W., Raghava, S., Katiyar, A., Nowak, C., Xiang, T., Dong, D., Sun, J., Beck, A., Liu, H. (2019) Structure, heterogeneity and developability assessment of therapeutic antibodies. *MAbs.* 11(2), 239-264.

[12] Kang, X., Kutzko, J., Hayes, M., Frey D., (2013) Monoclonal antibody heterogeneity analysis and deamidation monitoring with high-perfomance cation-exchange chromatofocusing using simple, two component buffer systems. *Journal of Chromatography A.* 1283, 89-97

[13] Teshima, G., Li, M. X., Danishmand, R., Obi, C., To, R., Huang, C., Kung, J., Lahidji, V., Freeberg, J., Thorner, L., Tomic, M. (2011). Separation of oxidized variants of a monoclonal antibody by anion-exchange. *Journal of Chromatography A*, *1218*(15), 2091–2097.

[14] Beck, A., Wagner-Rousset, E., Ayoub, D., Van Dorsselaer, A., Sanglier-Cianferani, S. (2013) Characterization of Therapeutic Antibodies and Related Products. *Analytical Chemistry.* 85, 715-736.

[15] Ponniah, G., Nowak, C., Neill, A., Liu, H. (2017) Characterization of charge variants of a monoclonal antibody using weak anion exchange chromatography at subunit levels. *Analytical Biochemistry.* 520, 49-57.

[16] Du, Y., Walsh, A., Ehrick, R., Xu, W., May, K., & Liu, H. (2012). Chromatographic analysis of the acidic and basic species of recombinant monoclonal antibodies. *MAbs*.4(5), 578-585.

[17] Hermeling, S., Crommelin, D., Schelleckens, H., Jiskoot, W. (2004) Structure-Immunogenicity Relationships of Therapeutic Proteins. *Pharmaceutical Research* 21(6), 897-903.

[18] Seedhara, A., Cordoba, A., Zhu, Q., Wkong, J., Liu, J. (2012) Characterization of the isomerization products of aspartate residues at two different sites in a monoclonal antibody. *Pharmaceutical Research,* 29(1), 187-197.

[19] Haverick, M., Mengisen, S., Shameem, M., Ambrogelly, A. (2014) Separation of mAbs molecular variants by analytical hydrophobic interaction chromatography HPLC: Overview and applications. *MAbs*. 6(4), 852-858.

[20] Chumsae, C., Gaza-Bulseco, G., Sun, J., Liu, H. (2007) Comparison of methionine oxidation in thermal stability and chemically stressed samples of a fully human monoclonal antibody. *Journal of chromatography B Analytical Technologies in the biomedical and life sciences*, 850(1-2), 285-294.

[21] Pan, H., Chen, K., Chu, L., Kinderman, F., Apostol, I., Huang, G. (2009) Methionine oxidation in human IgG2 Fc decreases binding affinities to protein A and FcRn. *Protein Science.* 18(2), 424-433

[22]   van de Bovenkamp, F., Hafkenscheid, L., Rispens, T., Rombout,Y. (2016) The Emerging Importance of IgG Fab Glycosylation in Immunity. *The Journal of Immunology*.196(4), 1435-1441.

[23]   Boune, S., Hu, P., Epstein, A., Khawli, L. (2020) Principles of N-Linked Glycosylation Variations of IgG-Based Therapeutics: Pharmacokinetic and Functional Considerations. *Antibodies*. 9(2), 22

[24]   Mauko, L., et al., (2011) Glycan profiling of monoclonal antibodies using zwitterionic-type hydrophilic interaction chromatography coupled with electrospray ionization mass spectrometry detection. *Analytical Biochemistry*. 408(2), 235-241

[25]   Doherty, M., et al., High-throughput quantitative N-glycan analysis of glycoproteins. Methods Mol Biol, 2012. 899: p. 293-313.

[26]   Hamm, M., Y. Wang, and R.R. Rustandi, Characterization of N-Linked Glycosylation in a Monoclonal Antibody Produced in NS0 Cells Using Capillary Electrophoresis with Laser-Induced Fluorescence Detection. Pharmaceuticals (Basel), 2013. 6(3): p. 393-406.

[27]   Alvarez, M., et al., On-line characterization of monoclonal antibody variants by liquid chromatography-mass spectrometry operating in a two-dimensional format. Anal Biochem, 2011. 419(1): p. 17-25.

[28]   Zhang, L., Luo, S., Zhang, B. (2016) Glycan analysis of therapeutic glycoproteins. *MAbs*. 8(2), 205-215.

[29]   Planinc, A., Bones, J., Dejaegher, B., Van Antwerpen, P., Delporte, C. (2016) Glycan characterization of biopharmaceuticals: Updates and perspectives. *Analytica Chimica Acta*. 921, 13-27

[30]   Bupp, C., Schwartz, C., Wei, B., Wirth, M., (2021) Protein-induced Conformational Change in Glycan Decreases Resolution of Glycoprotein in Hydrophilic Interaction Liquid Chromatography. Journal of Separation Science. 44(8), 1581-1591.

[31]   Zhang, T., et al., Identification and characterization of buried unpaired cysteines in a recombinant monoclonal IgG1 antibody. Anal Chem, 2012. 84(16): p. 7112- 23.

[32]   Liu, H., May, K. (2012) Disulfide bond structures of IgG molecules. *MAbs*. 4(1), 17-23.

[33]   Robotham, A., Kelly, J. Detection and quantification of free sulfhydryls in monoclonal antibodies using maleimide labeling and mass spectrometry. *MAbs*. 11(4), 757-766.

[34]   Zhang, W., Marzilli, L., Rouse, J., Czupryn, M. (2002) Complete disulfide bond assignment of a recombinant immunoglobulin G4 monoclonal antibody. *Analytical Biochemistry*. 311(1), 1-9.

[35]   Moritz, B., Strack, J, O. (2017) Assessment of disulfide and hinge modifications in monoclonal antibodies. *Electrophoresis*. 38(6), 769-785.

[36]   Nikolin, B., Imamović, B., Medanhodzić-Vuk, S., Sober, M. (2004) High perfomance liquid chromatography in pharmaceutical analyses. *Bosnian journal of basic medical sciences.* 4(2): 5-9.

[37]   Liu, H., Ma, J., Wnter, C., Bayer, R. (2010) Recovery and purification process development for monoclonal antibody production. *MAbs.* 2(5): 480-499.

[38]   Giddings, J.C., Unified separation science. 1991, New York: Wiley. xxiv, 320 p.

[39]   Olah, E., et al., Comparative study of new shell-type, sub-2 micron fully porous and monolith stationary phases, focusing on mass-transfer resistance. *J Chromatography A*, 2010. 1217(23): p. 3642-53.

[40]   Garcia-Canas, V., B. Lorbetskie, and M. Girard, Rapid and selective characterization of influenza virus constituents in monovalent and multivalent preparations using non-porous reversed-phase high performance liquid chromatography columns. *J Chromatography A*, 2006. 1123(2): p. 225-32.

[41]   Bell, D., Majors, R. (2015) Current State of Superficially Porous Particle Technology in Liquid Chromatography. *LCGC North America.* 33(6): 2-9

[42]   Spudeit, D.A., et al., Superficially porous particles vs. fully porous particles for bonded high performance liquid chromatographic chiral stationary phases: isopropyl cyclofructan 6. *J Chromatography A*, 2014. 1363: p. 89-95.

[43]   Gritti, F., et al., Evaluation of the kinetic performance of new prototype 2.1mmx100mm narrow-bore columns packed with 1.6mum superficially porous particles. *J Chromatography A*, 2014. 1334: p. 30-43.

[44]   Gritti, F. and G. Guiochon, Rapid development of core-shell column technology: accurate measurements of the intrinsic column efficiency of narrow-bore columns packed with 4.6 down to 1.3 mum superficially porous particles. *J Chromatography A*, 2014. 1333: p. 60-9.

[45]   Wagner, B., Schuster, S., Boyes, B., Shields, T., Miles, W., Haynes, M., Moran, R., Kirkland, J., Shure, M. (2018) Superficially porous particles with 1000 Å pores for large biomolecule high performance liquid chromatography and polymer size exclusion chromatography. *Journal of Chromatography A.* 1489: 75-85

[46]   Greasley, S., Page, S., Sirovica, S., Chen, S., Martin, R., Riveiro, A., Hanna, J., Porter, A., Jones,J. (2016) Controlling particle size in the Stöber process and incorporation of calcium. *Journal of Colloid and Interface Science.* 469: 213-223.

[47]   Cao, X. (2015) Liquid Chromatographic Separation of Therapeutic Monoclonal Antibodies with SUbmicrometer Particles (Doctoral Dissertation)

1.6   Figures
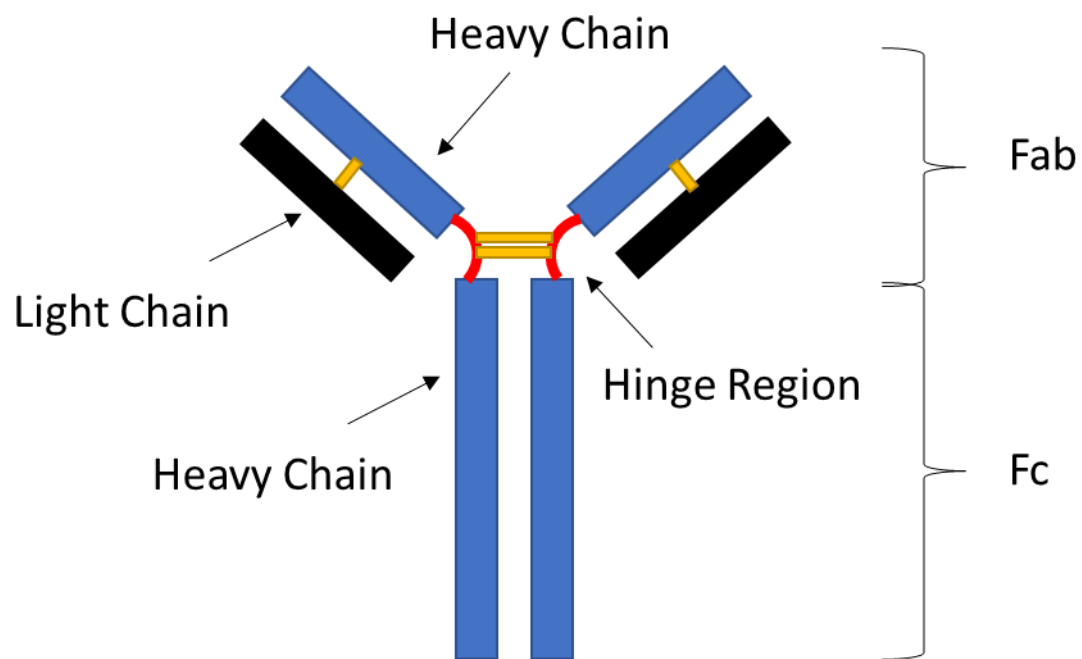
Figure 1. 1. Monoclonal antibody structure.

$$\text{Efficiency} \qquad \text{Selectivity}$$

$$R_S = \left[\frac{\sqrt{N}}{4}\right] * \left[\frac{\alpha - 1}{\alpha}\right] * \left[\frac{k}{k+1}\right]$$

Figure 1. 2 Equation for resolution defined by column efficiency and selectivity.

$$H = a \cdot d_p + 2\gamma D/v + c_m \cdot (d_p^2/2D) \cdot v + c_p \cdot (d_p^2/2D) \cdot v + c_s \cdot v$$
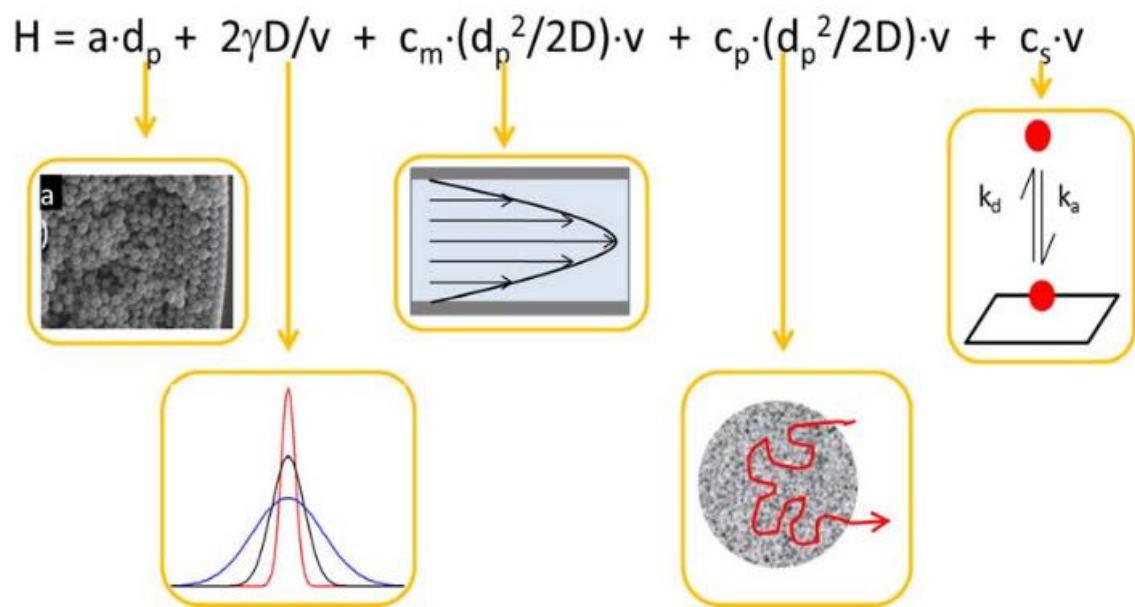
Figure 1. 3 Van Deemter equation with descriptors. (47)

Fully Porous   **Superficially Porous**   **Nonporous**
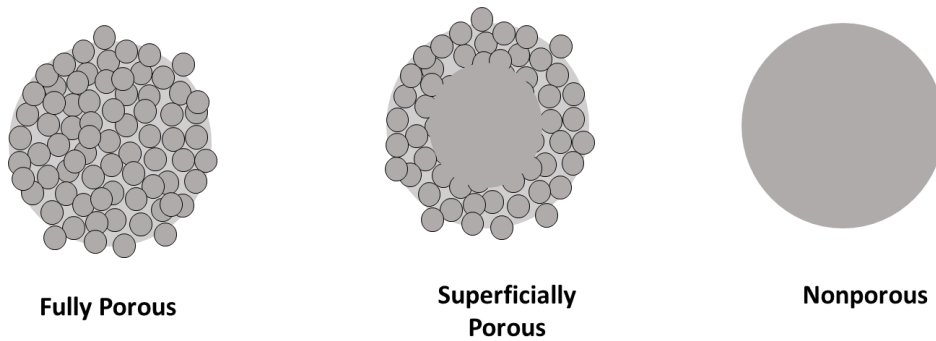
Figure 1. 4 Illustrations of the three major silica particle morphologies

CHAPTER 2.   DEVELOPMENT OF A WEAK ANION EXCHANGE STATIONARY PHASE FOR THE ANALYSIS OF AN IGG4 MONOCLONAL ANTIBODY CHARGE VARIANTS

2.1   Abstract

A novel weak anion exchange bonded phase was developed by using atom transfer radical polymerization of a copolymer containing 2-(dimethylaminoethyl)methacrylate – co – N-hydroxymethyl acrylamide on 1.5 um nonporous silica particles. Monomer concentrations were varied in order to optimize surface charge density during column development. Selectivity plots of ln(k) vs 1/√(ionic strength of mobile phase) of C-Terminal lysine variants of an IgG4 shows that a 2:1 charged to neutral monomer results in better selectivity than a fully charged surface. The lab made column was compared to a leading commercial column and was shown to have improved resolution of both basic and acidic charge variants of IgG4. The increase in resolution was contributed to improved efficiency from a decrease in particle size as well as greater selectivity. The commercial column was shown to interact with a larger surface area of the protein compared to the lab made column. A smooth polymer layer that controls surface charge by a blend of charged monomer and a neutral, hydrophilic monomer showed to have greater selectivity than a bonded phase consisting of spaced out charged ligands.

2.2   Introduction

Monoclonal antibodies (mAbs) have been used for treating numerous conditions including cancer (1,2) and autoimmune disease (2).The specificity and "magic bullet"(3) mindset of mAbs continue to make it one of the fastest growing areas in the pharmaceutical industry (4). Their complexity and high molecular weight (150 kDa) make for difficult characterization and present a very unique analytical challenge. Numerous posttranslational modifications can occur during production including those that lead to charge variants like sialyation(5), deamidation (6), oxidation (7), isomerization (8), succinimide formation (8), as well as incomplete C-terminal lysine clipping (9). Posttranslational modifications have the potential to lead to stability and efficacy issues and therefore must be characterized (7-9).

Ion exchange chromatography (IEC) is a common analytical technique used to help characterize and quantify charge variants by separating analytes based on their difference in isoelectric point (9,10). There are two types of IEC, anion exchange chromatography (AEX) and cation exchange chromatography (CEX). As CEX is commonly used for charge based separations of antibodies with basic pIs (11), AEX is commonly used for the separation of antibodies with neutral to acidic pIs (12). As more acidic IgG4 mAbs and fusion proteins continue to be developed (13) , improving AEX columns becomes more important.

Ion exchange resins can be either polymer or silica based with polymer being the most common (14). Polymeric supports usually consist of a polymeric poly(divinylbenzene) bead coated in a hydrophilic polymer with charged ligands extending off of the surface. (15) Polymer stationary phases have the advantage of having a wider pH range than silica supports which can suffer from hydrolysis of siloxane bonds in more basic environments (16) Silica provides better mechanical stability than polymer supports, which can allow for higher flow rates and better column to column reproducibility. High pressure separations of proteins in IEC have been shown to induce confirmational changes resulting in nonnative separations, and therefore are usually run under low pressure conditions (17). The less mechanical stability, and use of nonporous particles, means most IEC columns consist of large (10 or 5 um) particles and long (25 cm) columns to increase the number of theoretical plates without damaging the polymer based packed beds. The use of smaller particles would greatly improve the mass transfer term resulting in more efficient separations (18), so the use of a more mechanically stable silica support could allow for the use of smaller particles and improve AEX separations of monoclonal antibodies.

In this study, a novel weak anion exchange stationary phase (WAX) has been synthesized by surface initiated atom transfer radical polymerization (SI-ATRP). A copolymer containing 2-(dimethylaminoethyl) methacrylate (DMAEMA) and N-hydroxymethyl acrylamide (HMAM) was grown on 1.5 um nonporous silica nanoparticles. To study the effect of charge density on the surface, HMAM was used as a spacer molecule and the ratio between the two monomers was optimized. New stationary phase packed in a 50 x 2.1 mm column and compared to a leading commercial column consisting of 10 um polymer beads in a 250 x 2 mm column in the separation of an IgG4. Selectivity of bonded phases are independent of particle size and was studied using a retention mechanism formula developed by Ståhlberg (19-21) and used to help compare columns independent of particle size. C-Terminal lysine variants are commonly

27

characterized to determine manufacturing reproducibility (22), and are therefore used in this study to construct selectivity plots.

2.3. Theory

Ståhlberg (20) showed the retention of proteins in IEC can be represented by equation 1,

$$\ln(k) = \frac{(A_p\,\sigma_p)}{\sqrt{(F(2RT)\varepsilon_o\varepsilon_r)}} * \frac{1}{\sqrt{I}} + \ln(\Phi) \qquad (1)$$

where k is the retention factor, A_p is the area of the analyte that interacts with the stationary phase, σ_p is the charge density of the protein, F is faradays constant, R is the gas constant, ε_o is the permittivity of a vacuum, ε_r is the dielectric constant of the medium, I is the ionic strength of the mobile phase, Φ is the phase ratio. This linear relationship between the ln(k) vs $\frac{1}{\sqrt{I}}$ allows for selectivity comparisons between bonded phases (21) with $A_p*\sigma_p$ representing the slope and $\ln(\Phi)$ representing the intercept. Ionic interactions are long range forces, therefore the phase ratio needs to reflect not only bonded phase surface area, but also the distance at which the analyte feels ionic interactions in the mobile phase. Equations 2 describes Φ for ion exchange bonded phases with this characteristic width of absorption,

$$\Phi = \frac{A_s*b}{V_o} \qquad (2)$$

where A_s is the surface area of the bonded phase that interacts with the charged analyte, V_o is the column dead volume, and b is the characteristic width of adsorption. The b term describes the length of distance the analyte feels the interaction away from the bonded phase and is described in equation 3,

$$b = 2 * \left(\frac{\ln(2)RT\varepsilon_o\varepsilon_r \left(\frac{1}{\sigma_p{}^2} - \frac{1}{\sigma_s{}^2} \right)}{A_p*\kappa} \right) \qquad (3)$$

Where σ_s is the charge density of the surface, and κ is the inverse debye length. By comparing slopes and intercepts between bonded phases, one can begin to understand the difference in interactions taking place between the analyte and the bonded phase. This is used here to describe the difference in analyte interaction with various bonded phase and explain differences in resolution.

2.4.   Experimental

2.4.1   Chemicals and materials

SiO$_2$ nanoparticles (1.5 um in diameter) were purchased from Superior Silica. (Chandler, AZ) DMAEMA, HMAM, sodium L-ascorbate, and ammonium acetate (98%) were purchased from Sigma-Aldrich (St. Louis, MO). Stainless steel tubings, ferrules and internal nuts were purchased from Valco Instruments (Houston, TX). Stainless steel columns, frits, and end caps were purchased from Idex (Oak Harbor, WA). 2-(chloromethylphenylethyldimethyl) chlorosilane and trimethylchlorosilane were purchased from Gelest (Morrisville, PA). Copper(II) Chloride (99%) was purchased from Acros Organics (Morris Plains, NJ). Tris (2-dimethylaminoethyl) amine (Me$_6$TREN) was purchased from Alfa Aesar (Tewksbury, MA). Acetonitrile, ethanol, acetic acid, and ammonium hydroxide were purchased from Fischer Scientific (Pittsburg, PA). Millipore water (18.2 OHMS) was provided in house by (name of water system). Particle morphologies were imaged used an FEI Tecnai G2 20 transmission electron microscope (TEM).

Carboxypeptidase B and digestion buffer were purchased from G-Biosciences (St. Louis, MO). Ovalbumin and BSA were purchased from Sigma-Aldrich (St. Louis, MO) and a pharmaceutical grade IgG4 monoclonal antibody was provided by Eli Lilly (Indianapolis, IN). All samples were diluted with the low salt buffer (20 mM) used during the indicated separation to the desired concentration.

2.4.2   Stationary phase preparation

1.5 um in diameter silica particles were heat treated at 600 °C three times for 12 hours each rinsing with 1:1 water and ethanol between each treatment. Following the third heat treatment, the particles were heated to 1050°C for 3 hours. Particles were then rehydroxylated by refluxing in 1.5 M nitric acid for 16 hours. Particles were then rinsed with water until neutral pH, and dried in a vacuum oven. The rehydroxylated particles were then suspended in dry toluene containing 2% (v/v) chloromethylphenylethyldimethyl chlorosilane and 0.1% (v/v) butylamine. Particles were refluxed under nitrogen for 3 hours. After 3 hours, trimethylchlorosilane 2% (v//v) was added without cooling down the system and was refluxed for 3 hours. Particles were then rinsed in toluene two times followed by one rinse with ethanol before vacuum drying.

SI-ATRP was performed on the initiated silica particles. In short, 0.5 grams of initiated particles were suspended under nitrogen in 7.5 mL ethanol. 1.2 mL of 48% N-Hydroxymethyl acrylamide solution was added to 9.2 mL of water and then added to the particle suspension. 0.040g $CuCl_2$, 80 uL of Me_6TREN, and 2.5 mL water were sonicated together and added to the particle suspension. 2.1 mL DMAEMA was then added to the solution and the solution was nitrogen purged for 5 min. A nitrogen balloon was added and the solution was placed in 35 °C water bath. After 10 min, 0.020 ug sodium ascorbate was mixed with 2.5 mL water and injected into the solution. Reaction went for 30 minutes followed by three rinses with water.

0.27 g of particles were suspended in 2.5 mL of water which was then packed into a stainless steel column (5.0 cm x 2.1 mm) using a constant pressure pump (Chrom Tech Inc. Apple Valley, MN) with 30% ethanol/ 70% water under sonication as described in previous work (24). The hydrophilic copolymer bonded phase is covered by an issued patent. (25)

2.4.3 Chromatographic Conditions

A Waters Acquity I-Class UPLC system (Waters Corporation, Milford, MA) was used with an inline PDA detector with detection wavelength of 230 nm. Solvent A was 20 mM ammonium acetate and solvent B was 300 mM ammonium acetate. Solvent A and B were adjusted to the same pH with dilute ammonium hydroxide. The commercial column used in this study was a ProPac WAX-10 weak anion exchange column (250 mm x 2 mm) from Thermo Scientific (Waltham, MA). Flow rate were 0.1 mL/min with 8 ug injected..

2.5 Results and Discussion

2.5.1 pH optimization

DMAEMA is used as the weak anion exchange functional group with a pka of 8.6 (figure S1) (26). To study the effect of charge density on the surface, HMAM (figure S1) was added in various ratios to reduce the charge density on the surface. The total concentration of monomer used during the ATRP reactions were kept constant, as well as reaction time to control the polymer thickness as best as possible.

Solvent pH has been shown to impact the resolution of weak anion exchangers (26,27) by varying the total charge on the surface. The effect of pH was examined using a lab made column

made using 2 parts DMAEMA (figure 2.1) and 1 part HMAM (figure 2.1) during the polymerization for the separation of IgG4 (Figure 2.4). The pka of DMAEMA is pH 8.6 and pI of this IgG4 is estimated to be around pH 5.0, therefore pH 7.0 was chosen as the lowest pH to ensure that both the surface and protein are fully charged. The effect of charge density on the surface was explored by increased pH to optimize the separation.

A pH increases, retention decreases which would be expected because of the decrease in charge caused by approaching the pka of DMAEMA. Resolution improves as you increase pH between 7.0 and 8.0, followed by very little retention and resolution and pH 8.5. The lower retention indicates very little surface charge which would be expected around the pka of DMAEMA. pH 8.0 was chosen as the optimal pH and was used to compare columns here on out.

2.5.2 Column charge density optimization

Charge density optimization was performed by varying ratios of DMAEMA and HMAM during the polymerization reaction. Three ratios were tested 1:1, 2:1, and 1:0 of DMAEMA:HMAM. 1:1 DMAEMA:HMAM reaction showed poor resolution and broad peaks presumable from increased hydrophobic interactions resulting in slower mass transfer (figure 2.2). Therefore the 2:1 and DMAEMA only columns were compared.

Figure 2.5 shows the comparison of the DMAEMA only column, referred to as fully charged, and 2:1 DMAEMA:HMAM column, referred to as the blend column, using the same gradient at pH 8.0. Interestingly it is seen that the blend column has greater resolution of minor charged species than the fully charged column. The reason for the increase in resolution was examined by comparing selectivity plots of both columns (figure 2.5) with the resulting slope and intercept data shown in table 2.1. The three major peaks represent 0, 1, and 2 C-terminal lysine variants, respectively, and was confirmed by treatment with carboxypeptidase B to cleave C-terminal lysine variants and is shown in figure 2.3. These C-terminal lysine variants were used to compare selectivity between columns. Figure 2.5 shows that the blend column has higher selectivity than the fully charged column. Selectivity, α, is defined by the ratio of retention factors for two peaks, represented here by the 0 C terminal lysine variant and 2 C terminal lysine variant peaks. Here α was determined at the ionic strength were k=5 for the 0 C-terminal lysine variant. The slectivities are shown to be 3.01 and 2.02 for the blend and fully charged column

respectively. Since resolution is proportional to 1-α, resolution is doubled in the blend column compared to the fully charged column.

Table 2. 1 Slopes and intercepts of selectivity plots in figure 2.5b

Slope	2 C terminal lysines	1 C Terminal lysines	0 C terminal lysines
Fully charged column	2.35 ± 0.03	2.55 ± 0.04	2.94 ± 0.04
Blend column	2.82 ± 0.02	3.14 ± 0.02	3.91 ± 0.03
Intercept			
Fully charged column	-4.79 ± 0.10	-5.07 ± 0.11	-5.65 ± 0.11
Blend column	-6.27 ± 0.06	-6.73 ± 0.06	-7.79 ± 0.08

The slopes and intercepts of both columns were compared to try and explain this increase in selectivity. The slopes, which is proportional to A_p and $\sigma_{p,}$ (equation 1) for both columns are close to one another with the blend columns being slightly greater than the fully charged column. A possible explanation is a greater increase in protein interaction in the blend column from the protein partly submerging into the more hydrophilic surface. DMAEMA becomes a fairly hydrophobic monomer if it is deprotonated. The increase in hydrophobicity might hinder the IgG4 from entering the polymer, whereas the blend column contains HMAM, a more hydrophilic monomer, making it more favorable for the protein to enter the polymer layer, increasing the area of the protein interacting with the stationary phase. The intercept of the blend column is lower than that of the charge column. This is to be expected because the lower surface charge density would result in a smaller b term (equation 3) which would result in a smaller Φ and a lower intercept. From this it was determined that the blend column shows the greatest resolution and will be used to compare to a leading commercial column.

2.5.3   IgG4 separation comparison with commercial column

After charge density optimization, a comparison was made with a leading commercial column with particle size of 10 um and column dimensions of 2 x 250 mm. Figure 2.6 shows a comparison of the IgG4 separation between the two columns. The blend column has greater resolution compared to the commercial column. The smaller particle size (1.5 um vs 10 um) would result in an increase in efficiency resulting in sharper peaks. The slectivities were again calculated at the ionic strength were k=5 for 0-C terminal lysine variant. The slectivities were calculated to be 1.33 and 3.01 for the commercial and blend columns respectively, which would

result in about a 5 times increase in resolution from selectivity between the blend column and the commercial column.

The slopes and intercepts of the selectivity plots are shown in table 2.2. The slopes for the blend column are a little more than 2 times smaller than the commercial column. This suggests that the commercial column is resulting in over two times the area of the protein interacting with the bonded phase. This could occur from the protein interacting in a three dimensional manor with multiple charged ligands spaced out from one another, instead of a interacting with the protein on a more planar level. Figure 2.7 shows TEM micrographs of the commercial and blend particles. The blend particle shows a smooth polymer surface whereas the commercial particle shows a rough surface that would be expected if the charged ligands are spaced out from one another. Using a "grafting to" approach (27) would lead to a lower density of charged monomer compared to the "grafting from" approach (28.) used to grow the blend particle.

Table 2. 2 Slopes and intercept values for the selectivity plots in figure 2.6b

Slope	2 C terminal lysine	1 C Terminal lysine	0 C terminal lysine
Commercial Column	6.75 ± 0.03	7.23 ± 0.02	7.91 ± 0.04
Blend Column	2.82 ± 0.02	3.14 ± 0.02	3.91 ± 0.03
Intercept			
Commercial Column	-14.96 ± 0.07	-15.67 ± 0.05	-16.56 ± 0.04
Blend Column	-6.27 ± 0.06	-6.73 ± 0.06	-7.79 ± 0.08

The intercept for the blend column is almost an order of magnitude smaller than the commercial column. This is expected because of the larger surface area from the smaller particle size compared to the commercial column. A_s is directly proportional to Φ (equation 2), and the decrease in particle size results in a larger surface area, increasing the intercept. The decrease in protein interaction also leads to a larger intercept because b is inversely proportional to A_p and therefore the lower area of interaction results in a larger intercept.

2.4   Conclusion

In this work a novel weak anion exchange copolymer stationary phase was developed by SI-ATRP of DMAEMA and HMAM on 1.5 um nonporous silica. The surface charge density was optimized to show that a 2:1 DMAEMA:HMAM monomer ratio showed the greatest selectivity of IgG4 C-terminal lysine variants. A 5 cm column of the new bonded phase showed greater

resolution of IgG4 charge variants than a commercial 25 cm column. The smaller particle size (1.5 um vs 10 um) resulted in a greater efficiency and the stationary phase was shown to have greater selectivity for the separation of C-terminal lysine variants than the commercial column. Selectivity plots showed more than twice the area of interaction between the protein and the commercial columns bonded phase than the blend column. TEM of both particles showed a smooth polymer layer for the blend column, and a rough, bumpy layer for the commercial column. This suggests the commercial column was made using a grafting to approach, resulting in the protein being able to interact with the bonded phase from multiple sides, compared to one side with the blend column. The stronger interaction leads to less selectivity. Having a smooth, dense polymer layer and using a neutral spacer molecule to control charge density was shown to allow for better selectivity than spacing out charged ligands on a surface.

2.5 References

[1]   A. Scott, J. A. (2012). Monoclonal antibodies in cancer therapy. *Cancer Immunity, 12*, 14

[2]   Hafeez, U., Gan, H. K., & Scott, A. M. (2018, August 1). Monoclonal antibodies as immunomodulatory therapy against cancer and autoimmune diseases. *Current Opinion in Pharmacology*.

[3]   Brodsky, F. M. (1988). Monoclonal Antibodies as Magic Bullets. *Pharmaceutical Research: An Official Journal of the American Association of Pharmaceutical Scientists*.

[4]   Lu, R. M., Hwang, Y. C., Liu, I. J., Lee, C. C., Tsai, H. Z., Li, H. J., & Wu, H. C. (2020, January 2). Development of therapeutic antibodies for the treatment of diseases. *Journal of Biomedical Science*.

[5]   Higel, F., Seidl, A., Sörgel, F., & Friess, W. (2016, March 1). N-glycosylation heterogeneity and the influence on structure, function and pharmacokinetics of monoclonal antibodies and Fc fusion proteins. *European Journal of Pharmaceutics and Biopharmaceutics*.

[6]   Weitzhandler, M., Farnan, D., Horvath, J., Rohrer, J. S., Slingsby, R. W., Avdalovic, N., & Pohl, C. (1998). Protein variant separations by cation-exchange chromatography on tentacle-type polymeric stationary phases. *Journal of Chromatography A* 828, 365–372.

[7]   Khawli, L. A., Goswami, S., Hutchinson, R., Kwong, Z. W., Yang, J., Wang, X., … Motchnik, P. (2010). Charge variants in IgG1: Isolation, characterization, in vitro binding properties and pharmacokinetics in rats. *MAbs*, *2*(6), 613–624.

[8]   Sreedhara, A., Cordoba, A., Zhu, Q., Kwong, J., Liu J. (2012) Characterization of isomerization products of aspartate residues at two different sites in monoclonal antibody. *Pharmaceutical Research.* 29(1) 187-197.

[9]   Beck, A., Wagner-Rousset, E., Ayoub, D., Van Dorsselaer, A., & Sanglier-Cianférani, S. (2013). Characterization of therapeutic antibodies and related products. *Analytical Chemistry*.

[10]   Harris, R. J., Kabakoff, B., Macchi, F. D., Shen, F. J., Kwong, M., Andya, J., Shire, S., Bjork, N., Topal, K., Chen, A.,(2001). Identification of multiple sources of charge heterogeneity in a recombinant antibody. *Journal of Chromatography B Biomedical Sciences and Applications*, *752*(2), 233–245

[11]   Vlasak, J. and R. Ionescu, (2008,) Heterogeneity of Monoclonal Antibodies Revealed by Charge-Sensitive Methods. *Current Pharmaceutical Biotechnology.* 9(6), 468-481.

[12]   Teshima, G., Li, M. X., Danishmand, R., Obi, C., To, R., Huang, C., Kung, J., Lahidji, V., Freeberg, J., Thorner, L., Tomic, M. (2011). Separation of oxidized variants of a monoclonal antibody by anion-exchange. *Journal of Chromatography A*, *1218*(15), 2091–2097.

[13]   Strohl, W. (2018) Current progress in innovative engineered antibodies. *Protein Cell.* 9(1), 86-120.

[14]   Nordborg, A., and E. Hilder., (2009) Recent advances in polymer monoliths for ion-exchange chromatography. *Analytical and Bioanalytical Chemistry.* 394, 71-84

[15]   Muller, W., (1990) New Ion-Exchanges for the Chromatography of Biopolymers. *Journal of Chromatography,* 510, 71-84

[16]   Ducom, G., Laubie, B., Ohannessian, A., Chottier, C., Germain, P., Chatain, V., Hydrolysis of polydimethoylsiloxane fluids in controlled aqueous solutions. (2013) *Water Science and Technology.* 68(4), 813-820.

[17]   Kristl, A., Lokošek, P., Pompe, M., Podgornik, A. (2019) Effect of pressure on the retention of macromolecules in ion exchange chromatography. *Journal of Chromatography A*.1597, 89-99.

[18]   MacNair, J., Lewis, K., Jorgenson, J. Ultrahigh pressure reversed-phase liquid chromatography in packed capillary columns. *Analytical Chemistry*, 1997. 69(6), 983-989.

[19]   Ståhlberg, J., Jönsson, B., & Horváth, C. (1991). Theory for Electrostatic Interaction Chromatography of Proteins. Analytical Chemistry, 63(17), 1867–1874. https://doi.org/10.1021/ac00017a036

[20]   J Stahlberg., (1999) Retention models for ions in chromatography. *Journal of Chromatography A.* 855, 3-55.

[21]   Bengt, J., and J Stahlberg., (1999) the electrostatic interaction between a charged sphere and an oppositely charged planar surface and its application to protein adsorption *Colloids and Surfaces B: Biointerfaces. .* 14, 67-75.

[22]   Du, Y., Walsh, A., Ehrick, R., Xu, W., May, K., & Liu, H. (2012). Chromatographic analysis of the acidic and basic species of recombinant monoclonal antibodies. *MAbs*.4(5), 578-585.

[23]   Zhang, Z. R., Wu, Z., Wirth, M. J., Polyacrylamide brush layer for hydrophilic interaction liquid chromatography of intact glycoproteins. *J. Chromatogr. A* 2013, *1301*, 156-161 DOI: 10.1016/j.chroma.2013.05.076.

[24]   Mary J. Wirth, Y. H., Zhaorui Zhang, Protein chromatography matrices with hydrophilic copolymer coatings. USA patent publ. date 2017.

[25]   Laurence, J., Nelson, B., Ye, Q., Park, J., Spencer, P. (2014) Characterization of Acid-neutralizing Basic Monomers in Co-solvent Systems by NMR. *International Journal of Polymeric Materials* 63(7), 361-367.

[26]   Staby, A., Jensen, R., Bensch, M., Hubbuch, J., Dünweber, D., Krarup, J., Nielsen, J., Lund, M., Kidal, S., Hansen, T., Jensen, I. (2007) Comparison of chromatographic ion-exchange resins: VI. Weak anion-exchange resins. *Journal of Chromatography A*. 1-2(14), 29-94.

[27]   Koursos, V., van der Vegte, W., Grim, P., Hadziioannou, G. (1998) Isolated Polymer Chains vis Mixed Self-Assembled Monolayers: Morphology and Friction Studied by Scanning Force Microscopy. *Macromolecules*. 31, 116-123.

[28]   Matyjaszewski, K., Dong, H., Jakubowski, W., Pietrasik, J., Kusumo, A. (2007) Grafting from Surfaces for "Everyone": ARGET ATRP in the Presence of Air. *Langmuir*. 23, 4528-4532.

2.6 Figures
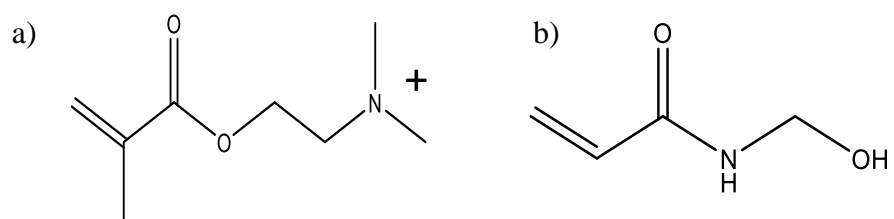
Figure 2. 1 Structure of monomers making up WAX copolymer a) DMAEMA b) HMAM
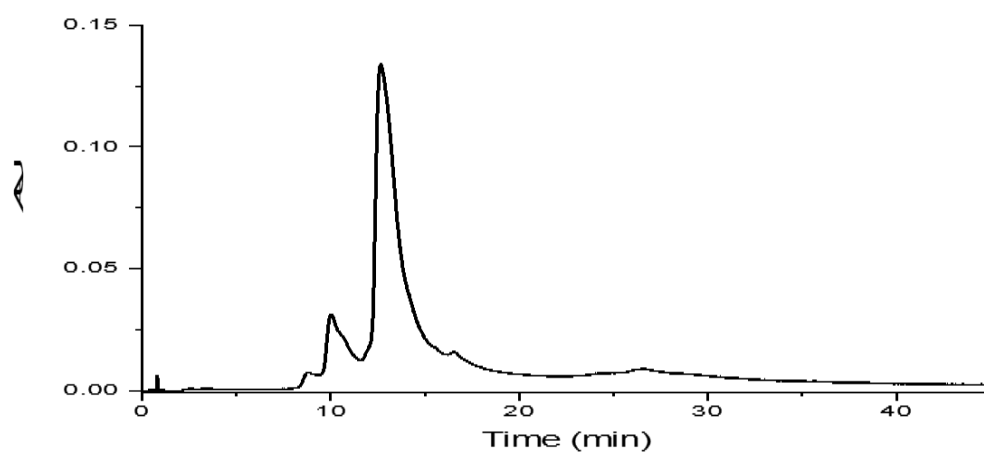
Figure 2. 2 Separation of IgG4 using 1:1 DMAEMA:HMAM column. 5-95% B in 40 min. Broad peaks represent poor resolution and resulted in no further experimentation.
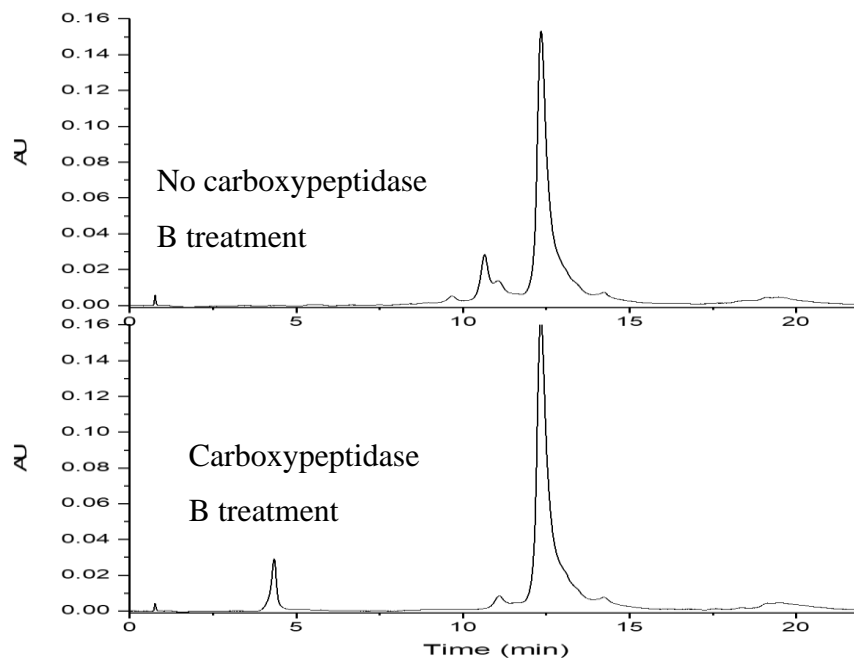
Figure 2. 3 Comparison of carboxypeptidase B treated IgG4 and native IgG4 using the lab made blend column. The disappearance of the first 2 major peaks after carboxypeptidase B treatment confirms the identity of the C-terminal lysine variants. 5-95% B in 20 min. 100uL/min.
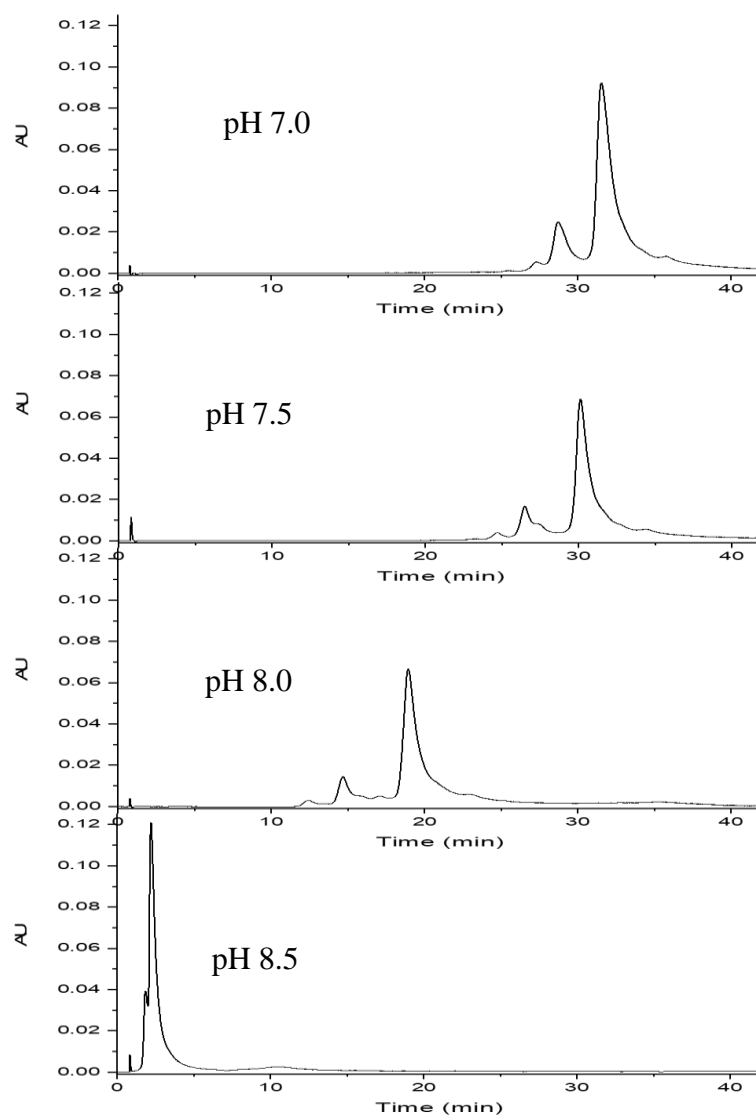
Figure 2. 4 pH comparison of IgG4 separation for the blend column at different pHs. As pH increase the charge density on the surface decreases resulting in less retention. 5-95% B in 40 min.
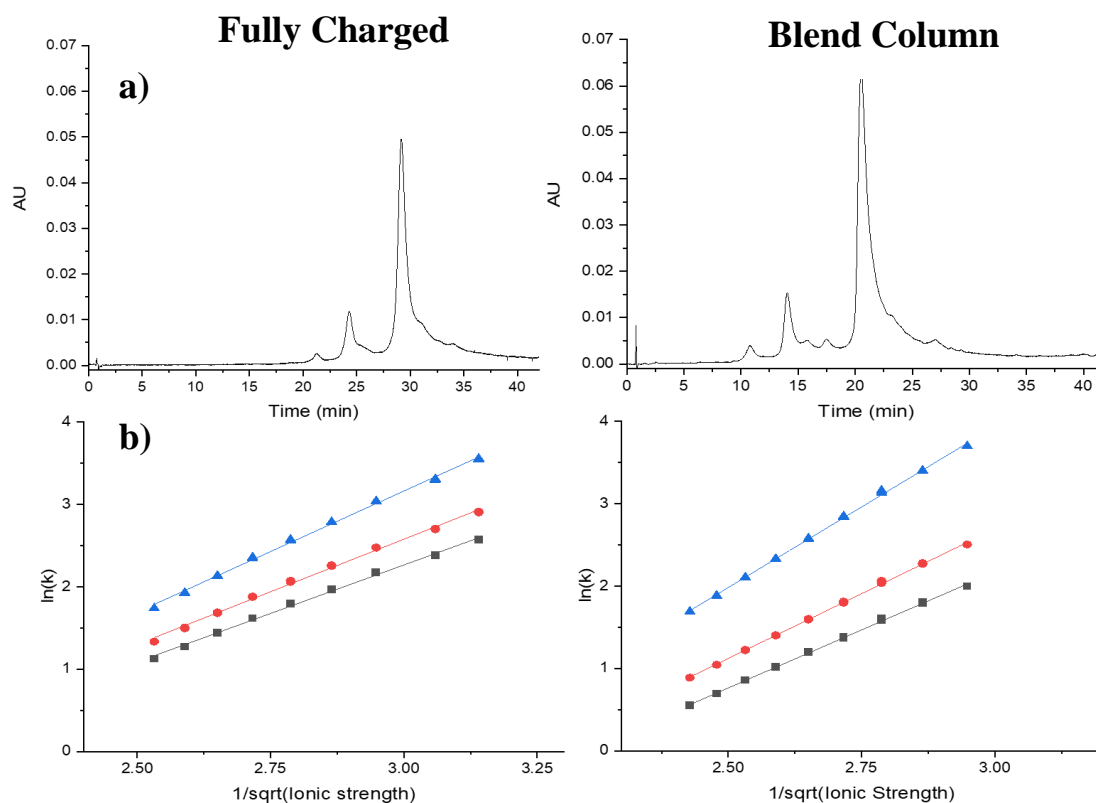
Figure 2. 5 a) Comparison of the fully charged column (left) and blend column (right) for the separation of IgG4. 10-60% B in 40 min. b) selectivity plots for fully charged column (left) and blend column (right). Blue, red, and grey lines represent 0, 1, and 2 C-terminal lysine variants respectively.
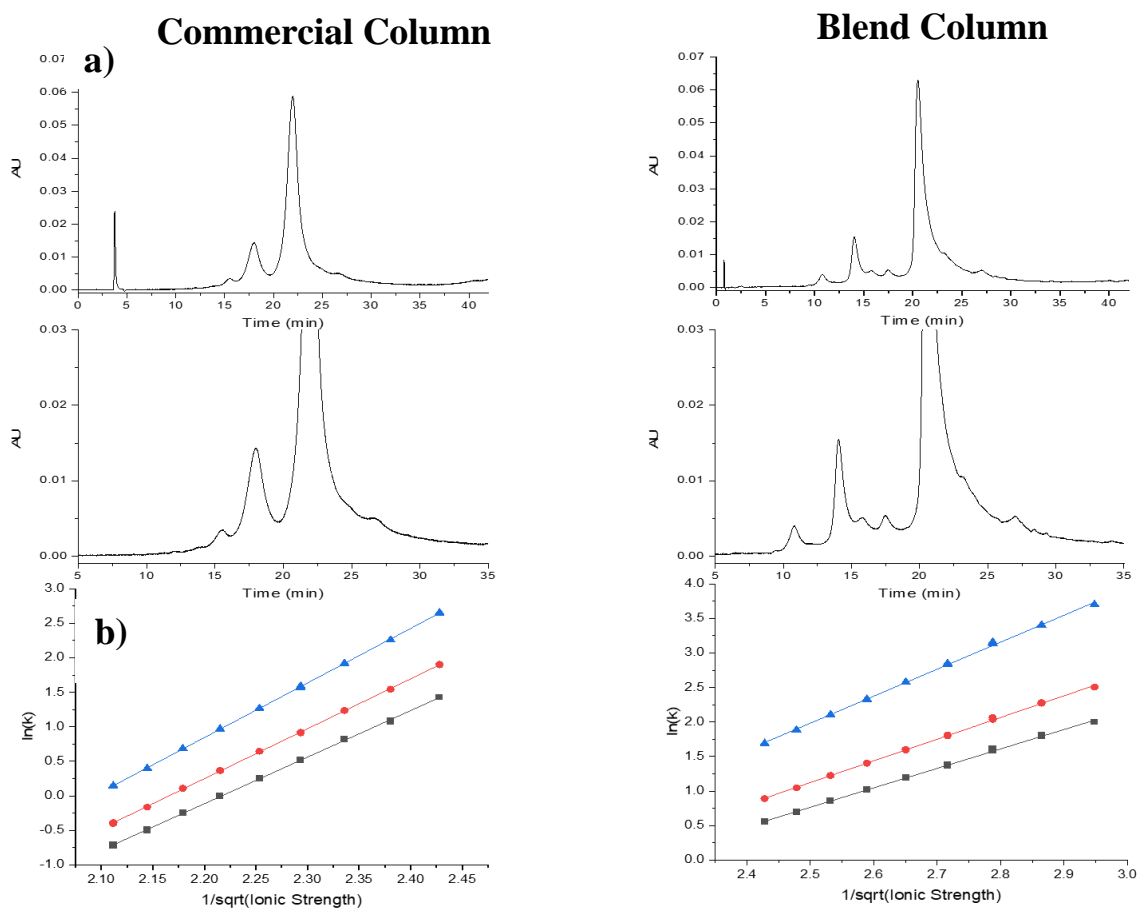
Figure 2. 6 a) IgG4 separation for the commercial column (left) and the lab blend column (right). Running conditions were 10-60% B for 40 min for the lab made column and 50-100% B in 40 min for the commercial column. A blown up chromatogram is shown below to help compare resolution. b) Selectivity plots for the separation of the commercial column (left) and the blend column (right). Blue, red, and grey lines represent 0, 1, and 2 C terminal lysine variants respectively.

Blend Particle   **Commercial Particle**
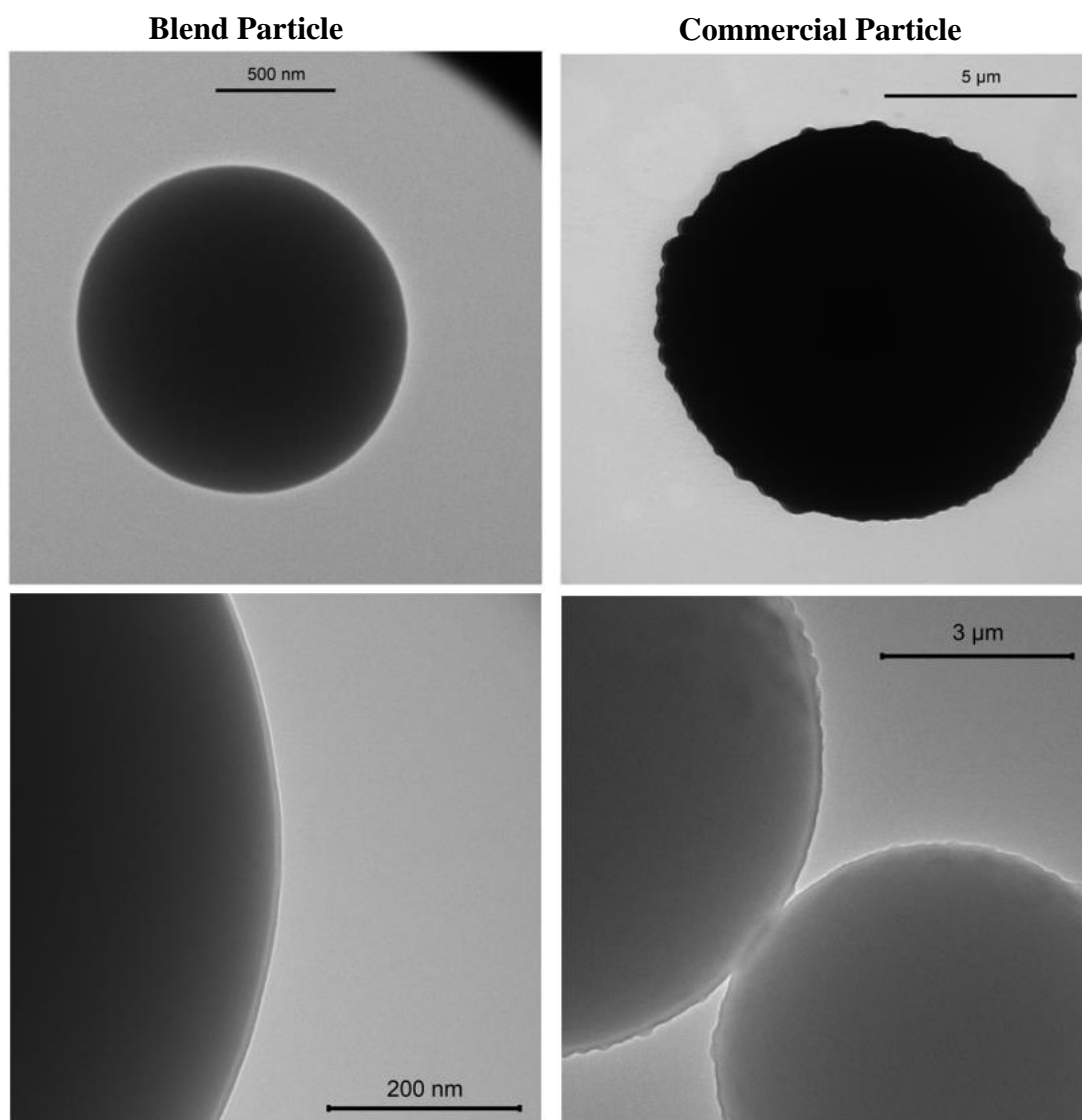
Figure 2. 7 TEM micrographs of blend particles (left) and commercial column particles (right). A smooth polymer layer of 7 nm can be seen for the blend column compared to a rough, undefined thickness for the commercial column

CHAPTER 3.   DEVELOPMENT OF A WEAK CATION EXCHANGE STATIONARY PHASE FOR THE ANALYSIS OF MONOCLONAL ANTIBODY CHARGE VARIANTS

3.1   Abstract

A novel weak cation exchange was developed using acrylic acid functionalized to silica nanoparticles. A smooth polymer layer of tertbutyl acrylate was grown on 1.5 um silica nanoparticles using atom transfer radical polymerization followed by hydrolysis to yield acrylic acid. Degree of hydrolysis was determined by contact angle measurements. Column performance was tested with the NIST IgG1 standard as well as an IgG1 and subsequent antibody drug conjugate (ADC) from AbbVie. A comparison with a leading commercial column showed only a slight difference in mAb resolution, but an increase in resolution in separating charge variants of the ADC with the commercial column showing limited elution of the ADC form the column. The more hydrophilic lab made column allowed for ADC charge variant analysis. While the ADC was able to elute from the column, slight hydrophobic interactions could still be observed indicating further column development or the addition of an organic solvent (10% acetonitrile) would be needed to further improve resolution.

3.2   Introduction

An increasing number of monoclonal antibodies (mAbs) are being continuously developed and given FDA approval every year (1). Characterization is of upmost importance because of various efficacy and safety concerns. Liquid chromatography has been shown to be a leading analytical technique in mAb characterization to help identify various posttranslational modifications. Charge variants can be caused by numerous post translational modifications including deamidation (2-6), isomerization (4-6), hydrolysis(5,6), racemization(5,6), C-terminal lysine clipping(5,6), glycosylation(5-7), and oxidation(8). The most common method to characterize these charge various is cation exchange chromatography (CEX) (9) because of the acidic isoelectric points of the more common IgG1 used for todays mAbs (10).

CEX is broken up into two distinct stationary phases; weak or strong cation exchange. Strong cation exchange (SCX) uses a highly acidic stationary phase whose surface charge is pH

independent. A common type of SCX contains a sulfate group (11). Weak cation exchange (WCX) on the other hand has a weakly acidic functional group where its surface charge is dependent on pH. These stationary phases have pKa values usually between 4 -5 and therefore surface charge decreases as you approach the pKa value. It has been shown that there is most often a difference in selectivity between a SCX and WCX column (12).

Within the mAb product class, antibody drug conjugates (ADCs) are an emerging subclass that is gaining significant traction. ADCs are mAbs with a conjugated cytotoxic drug linked to it allowed the cytotoxic payload to selectively target a surface of interest. This allows for site specific interaction of the toxic drug, reducing exposure to other sites and decreasing toxicity throughout the body (13). There are two conventional methods for drug conjugation of mAbs to form ADCs. First generation accomplished this through linkage of hydrazone linkers to random lysine residues. This does not allow for site specific linkage which can lead to efficacy and safety issues and is no longer the route of choice (10). Second generation ADC's conjugate the toxic drug through intermediate thiol linker resulting in a more site specific linkage leading to more controllable drug conjugation leading reducing the safety and efficacy concerns of the first generation (10). Drug conjugation usually requires an intermediate reaction step that may include reduction, reduction/reoxidation, or other reactions that modify a bifunctional linker for attachment. These reactions will include changes in pH, temperature, solvents, etc.. which may lead to posttranslational modifications not present on the initial mAb product (10). Being able to characterize not only the original mAb, but also the underlying the mAb after drug conjugation to understand how the reaction conditions affect the mAbs structure during after conjugation.

Current CEX columns consisting of polymeric supports may result in poor resolution of ADC separations because of unwanted hydrophobic interactions. Hydrophobic interactions will lead to peak broadening and lower resolution than is needed for characterization. Commercial polymer stationary phases have increased hydrophobicity than compared to silica particles leading to adhesion of the ADC resulting in lower efficient and subsequent lower percent recovery. Most commercial CEX use polymeric beads coated in a hydrophilic layer to reduce secondary hydrophobic interactions, but this coverage is not always complete and therefore can lead to a fairly hydrophobic surface resulting in unwanted secondary interactions and less efficient separations of ADCs.

In this work a novel WCX stationary phase was developed using an acrylic acid polymer on 1.5 um silica nanoparticles. Atom transfer radical polymerization (ATRP) was used to polymerize terbutylacrylate on the silica nanoparticles followed by hydrolysis leading to an poly(acrylic acid) polymer surface. This new WCX column was compared to a leading commercial column in the separation of NIST IgG1 standard, and a pharmaceutical mAb and subsequent ADC.

3.3   Experimental

3.3.1   Chemicals and materials

SiO_2 nanoparticles (1.5um in diameter) were purchased from Superior Silica. (Chandler, AZ) Terbutyl acrylate, sodium L-ascorbate, ammonium acetate (98%), ammonium bicarbonate (99%), trifluoroacetic acid (99%), and ammonium hydroxide (98%) were purchased from Sigma-Aldrich (St. Louis, MO). HPLC grade 2-propanol (IPA), dichloromethane (DCM), concentrated acetic acid (17.4 M), and 30% ammonium hydroxide were purchased from Fischer Scientific (Pittsburg, PA). Stainless steel tubings, ferrules and internal nuts were purchased from Valco Instruments (Houston, TX). Stainless steel columns, frits, and end caps were purchased from Idex (Oak Harbor, WA). 2- (chloromethylphenylethyldimethyl) chlorosilane and trimethylchlorosilane were purchased from Gelest (Morrisville, PA). Copper(II) Chloride (99%) was purchased from Acros Organics (Morris Plains, NJ). Tris (2-dimethylaminoethyl) amine (Me_6TREN) was purchased from Alfa Aesar (Tewksbury, MA) FabRICATOR was purchased from Genovis (Cambridge, MA). Ultrapure water (18 mΩ) was prepared with a Milli-Q Gradient in-lab purifier from Millipore (Burlington, MA).

NIST IgG1 standard was purchased from the National Institute for Standards and Technologies (Gaithersburg, MD) and a pharmaceutical grade IgG1 monoclonal antibody and subsequent ADC was provided by Abbvie (Lake Hill, IL).

3.3.2   Stationary Phase Preparation

1.5 um in diameter silica particles were heat treated at 600 °C three times for 12 hours each rinsing with 1:1 water and ethanol between each treatment. Following the third heat treatment, the particles were heated to 1050 °C for 3 hours. Particles were then rehydroxylated

by refluxing in 1.5 M nitric acid for 16 hours. Particles were then rinsed with water until neutral pH, and dried in a vacuum oven. The rehydroxylated particles were then suspended in dry toluene containing 2% (v/v) chloromethylphenylethyldimethyl chlorosilane and 0.1% (v/v) butylamine. Particles were refluxed under nitrogen for 3 hours. After 3 hours, trimethylchlorosilane 2% (v//v) was added without cooling down the system and was refluxed for 3 hours. Particles were then twice with toluene followed by one rinse with ethanol before vacuum drying.

SI-AGET ATRP was performed on the silicas surface as described previously. In short, 0.5 grams of initiated particles were suspended under nitrogen in 17.5 mL IPA. 3.7 mL of Tertbutyl acrylate solution was added to the particle suspension. 0.040g $CuCl_2$, 80 uL of Me_6TREN, and 1.9 mL water were sonicated together and added to the particle suspension. A nitrogen balloon was then added and solution was placed in 35 °C water bath. After 10 min, 0.020 ug sodium ascorbate was mixed with 1.9 mL water and injected into the solution. Reaction ran for 60 min, and solution was rinsed three times with IPA. The particles were then rinsed one time with DCM and then suspended in 40 mL of DCM. 4 mL of TFA was then added and the solution was stirred at room temperature for 18 hours. Particles were then rinsed twice with IPA, followed by three rinses with water and vacuum dried before packing.

0.27 g of particles were suspended in 2.5 mL of water which was then packed into a stainless steel column (5.0 cm x 2.1 mm) using a constant pressure pump (Chrom Tech Inc., Apple Valley, MN) using a 30% ethanol/ 70% water packing solution under sonication.

3.3.3   Chromatographic Conditions

A Waters Acquity I-Class UPLC system (Waters Corporation, Milford, MA) was used with an inline PDA detector to perform all chromatographic separations at a 230 nm wavelength detection.. Solvent A was 20 mM ammonium acetate adjusted to pH 5.0 with acetic acid. Solvent B was 140 mM ammonium acetate, 10 mM ammonium bicarbonate adjusted to pH 8.0 with ammonium hydroxide. All samples were diluted to indicated concentration using solvent A. The commercial column used in this study was a Propac WCX-10 weak action exchange column (25 cm x 2 mm) from thermo scientific (Waltham, MA).

3.3.4 Ides digestion of NIST mAb

NIST mAb was digested according to literature (15). In short, 200 ug of NIST mAb was diluted to 1 mg/mL in 200 uL of 50 mM Tris buffer pH 7.5. 200 ug of FabRICATOR Ides was added to the solution and placed in a 37 °C water bath for 30 minutes. Solution was spun in 10 kDa spin filter at 14,000 g's for 10 min. Sample was then placed in solvent A and spun again at 14,000 g's. Sample was then diluted to the desired concentration with solvent A.

3.4   Results and Discussion

3.4.1   Particle surface characterization

It has been shown that the tertbutyl group in tertbutyl acrylate polymer can go through acid hydrolysis using TFA to produce an acrylic acid surface (17-19). With this in mind, tertbutyl acrylate was grown on 1.5 um silica particles via SI-ATRP followed by acid hydrolysis and the polymer shell can be seen in figure 3.1. The smooth polymer layer is around 14 nm in length which should provide enough distance to prevent interaction of the protein with the negatively charged silica surface.

To determine the hydrolysis time needed for cleavage of the tertbutyl groups into carboxylic acids, a tensiometer was used to calculate contact angle of modified silicon wafers. Silicon wafers were modified using the same reaction conditions as the modified particles, followed by hydrolysis using the same conditions as the silica particles. Water was then dropped on the wafer and its contact angle was measured and results can be seen in table 3.1. No hydrolysis resulted in contact angle around 90° indicating the surface is highly hydrophobic which is characteristic of poly(tertbutyl acrylate) polymer (19). As hydrolysis time increases, the contact angle continues to decrease until it is so small that it was unable to be measured by the instrument. This indicates a highly hydrophilic surface and is expected from a poly(acrylic acid) surface(19). After 18 hours, it was seen that the contact angle increased again indicating the surface begins to have some hydrophobic character. This is characteristic of polymer cleaving from the surface and exposing the more hydrophobic moieties of the silica surface. This leads to the conclusion that 18 hours of hydrolysis was sufficient to convert tertbutyl acrylate to acrylic acid without exposing the silica surface.

Table 3. 1 Contact angle measurements of the hydrolysis of tert-butyl acrylate silicon wafers with 10% TFA in DCM. Measurements were done on the same wafer in triplicate. NA represents the angle was too small for the instrument to calculate.

Hours of Hydrolysis	Contact Angle	Average
0	90, 91, 89	90 $\pm$ 1
3	63, 62, 60,	62 $\pm$ 2
6	45, 43, 42	43 $\pm$ 2
9	40, 39, 38	39 $\pm$ 1
12	36, 36, 34	35 $\pm$ 1
15	15, 16, 14	15 $\pm$ 1
18	NA,NA,NA	NA
21	NA, 10, NA	10 $\pm$ NA
24	12, 14, 10	12 $\pm$ 2

3.4.2   mAb and ADC separation comparison with a commercial column

Particles were then packed into a 5 cm column and ran with mass spec compatible solvents to determine the separation efficiency of the polymer shell stationary phase. In order to determine locations of charge variants, Ides digesting can be performed to split the mAb into Fab and Fc/2 portions (15). Figure 3.2 shows the resulting chromatograms of an Ides digesting NIST mAb. The Fc portion elutes early in the separation because of the smaller analyte size (25 kDa) compare to the Fab (50 kDa). Examining just the Fc portion of the chromatogram, figure 3.2 shows the main charge variant containing multiple peaks in the lab made column compared to just one peak for the commercial column. The lab made column also allows for slightly better resolution of basic variants (later eluting species) than the commercial column. The two main variants are most likely C-Termianl lysine variants, which could be identified using a mass spectrometer with inline LC-MS because of the mass spectrometry compatible salts being used for the separation. A similar conclusion can be made when examining the separation of a mAb provided by Abbvie (figure 3.3). Both columns provide similar resolution with slight differences in selectivity, especially when comparing the earlier eluting species. This changes when you compare the separation of the subsequent ADC produced from that commercial mAb.

Figure 3.4 shows that the lab made column separates the charge variants of the ADC much better than the commercial column. The drug product and linker structure for the ADC is also shown in figure 3.4 and it is easy to see how the hydrophobic nature of the drug and linker can lead to hydrophobic interactions with a polymer surface. The percent recovery between the

two columns is vastly different with the lab made column having significantly higher than that of the commercial column. Hydrophobic interactions of the ADC are leading to minimal elution of from the column for the commercial column. In contrast, the lab made column has considerably less hydrophobic interactions leading to the conclusion that the lab made column surface is more hydrophilic than that of the commercial column. This hydrophilicity allows for the elution of the ADC unlike the commercial column

Overlaying the mAb and ADC for each column (Figure 3.5) it can be seen how the conjugation of the drug affects the charge profile of the analyte. The lab made column's major peak is shifted to earlier elution for the ADC compared with the mAb. This indicates that the ADC is more acidic than the underlying mAb after drug conjugation. This is most do to the drug molecule being conjugated to a cysteine residue, making the analyte less negative and resulting in a more acidic molecule. The major peak in the mAb separation is still present in the ADC separation indicating incomplete conjugation. The fact that there is only one new peak present in the ADC chromatogram compared to the mAb indicates a very narrow DAR range and the most common DAR of 2. Looking at the commercial column overlay (figure 3.5) the same conclusion can be made that hydrophobic interactions are too strong to allow for the elution of the ADC analyte and that only the unconjugated mAb elutes form the column, as seen by the overlapping peaks between mAb and ADC chromatograms.

The lab made column does improve the percent recover and resolution of ADC charge variant separations, but hydrophobic interactions are still taking place. Figure 3.5 shows that the mAb separation is able to separate more minor charge variants than the ADC separation. If the only difference between the two analytes is drug conjugation, these minor charge species should still be present, but the resolution of these species has decreased. This decrease in resolution leads me to believe that hydrophobic interactions are still occurring in the lab made column., just to a lesser extent than it is in the commercial column. More column optimization will need to happen in order to decrease the hydrophobic interaction. The addition of 10% organic, like acetonitrile, may also be using in the solvents to reduce this hydrophobic interaction and lead to better resoluiotn.

3.5   Conclusion

A new silica-polymer shell weak cation exchange stationary phase was developed and compared to a commercial column for the separation of mAbs and ADC. Tertbutyl acrylate was grown using ATRP and hydrolyzed using acid to leave acrylic acid on the surface as confirmed by TEM and contact angle measurements. The lab made 5 cm column showed comparable resolution and efficiency of that of a commercial column in the separation of the Ides digested NIST IgG1 and for the separation of an intact commercial mAb. The separation of the commercial ADC proved to be challenging for the commercial column because of unwanted hydrophobic interactions between that of the drug and the bonded phase. This resulted in low percent recovery and no charge based separation of the ADC. In contrast the lab made column was able to elute and separate charge variants of the ADC indicating that the lab made surface is more hydrophilic than that of the commercial column. The shift of the major peak of the ADC compared to the underlying mAb shows that the conjugation formed a more acidic analyte, most likely form conjugation with cysteine residues in the FC region. The major peak for the underlying mAb separation was still present in the ADC separation indicating the presence of unconjugated mAb species. More optimization will have to be done in the future to optimize the charge density of the bonded phase to provide even better resolution compared to the commercial column. This could be done by introducing a spacer polymer like what was presented in chapter 2 as well as further optimization of polymer thickness and density to help block unwanted silanol interactions.

3.6   References

[1]   Mullard, A. (2021) FDA approves 100th monoclonal antibody produce. *Nature Reviews Drug Discovery.* doi: https://doi.org/10.1038/d41573-021-00079-7.

[2]   Du, Y., Walsh, A., Ehrick, R., Xu, W., May, K., & Liu, H. (2012). Chromatographic analysis of the acidic and basic species of recombinant monoclonal antibodies. *MAbs*.

[3]   Kang, X., Kutzko, J., Hayes, M., Frey D., (2013) Monoclonal antibody heterogeneity analysis and deamidation monitoring with high-perfomance cation-exchange chromatofocusing using simple, two component buffer systems. *Journal of Chromatography A.* 1283, 89-97

[4]   Weitzhandler, M., Farnan, D., Horvath, J., Rohrer, J. S., Slingsby, R. W., Avdalovic, N., & Pohl, C. (1998). Protein variant separations by cation-exchange chromatography on tentacle-type polymeric stationary phases. *Journal of Chromatography A* 828, 365–372.

[5]   Khawli, L. A., Goswami, S., Hutchinson, R., Kwong, Z. W., Yang, J., Wang, X., … Motchnik, P. (2010). Charge variants in IgG1: Isolation, characterization, in vitro binding properties and pharmacokinetics in rats. *MAbs*, *2*(6), 613–624.

[6]   Gaza-Buleseco, G., Buleseco, A., Chumasa, C., Liu, H. (2008) Characterization of glycosylation state of a recombinant monoclonal antibody using weak cation exchange chromatography and mass spectrometry. *Journal of Chromatography B.* 862, 155-160

[7]   Higel, F., Seidl, A., Sörgel, F., & Friess, W. (2016, March 1). N-glycosylation heterogeneity and the influence on structure, function and pharmacokinetics of monoclonal antibodies and Fc fusion proteins. *European Journal of Pharmaceutics and Biopharmaceutics*.

[8]   Teshima, G., Li, M. X., Danishmand, R., Obi, C., To, R., Huang, C., Kung, J., Lahidji, V., Freeberg, J., Thorner, L., Tomic, M. (2011). Separation of oxidized variants of a monoclonal antibody by anion-exchange. *Journal of Chromatography A*, *1218*(15), 2091–2097.

[9]   Vlasak, J. and R. Ionescu, (2008,) Heterogeneity of Monoclonal Antibodies Revealed by Charge-Sensitive Methods. *Current Pharmaceutical Biotechnology.* 9(6), 468-481.

[10]   Beck, A., Goetsch, L., Dumontet, C., Corvaia, N. (2017) Strategies and challenges for the next generation of antibody-drug conjugates. *Nature Reviews Drug Discovery.* 16(5), 315-337.

[11]   Urmann, M., Graalfs, H., Joehnck, M., Jacob, L., Frech, C. (2010) Cation-exchange chromatography of monoclonal antibodies. *MAbs* 2(4), 395-404.

[12] Baek, J., Schwahn, A., Lin, S., Pohl, C., De Pra, M., Tremintin, S., Cook, K. (2020) New Insights into the Chromatography Mechanisms of Ion-Exchange Charge Variant Analysis: Dispelling Myths and Providing Guidance of Robust Method Optimization. *Analytical Chemistry.* 92(19), 13411-13419.

[13] Khongorzul, P., Ling, C., Khan, F., Ihasan, A., Zhang, J. (2020) Antibody-Drug Conjugates: A comprehensive Review. *Molecular Cancer Research.* 18(1), 3-19,

[14] Zhang Z., Zhou S., Han L., Zhang Q., Pritts W. (2019) Impact of linker-drug on ion exchange chromatography separation of antibody-drug conjugates. *MAbs* 11(6), 1113-1121.

[15] Vincents, B.; von Pawel-Rammingen, U.; Björck, L.; Abrahamson, M., Enzymatic (2004) Characterization of the Streptococcal Endopeptidase, IdeS, Reveals That It Is a Cysteine Protease with Strict Specificity for IgG Cleavage Due to Exosite Binding *Biochemistry-Us*, 43 (49), 15540-15549.

[16] Hutchinson, M., Hendricks, R., Lin, X., Olson, D., (2018) Chapter 40-Process Development and Manufacturing of Antibody-Drug Conjugates. *Biopharmaceutical Processing.* 813-836.

[17] Sütekin, D., Güven, O. (2020). Preparation of poly(tert-butyl acrylate)-poly(acrylic acid) amphiphilic copolymers via radiation-induced reversible addition–fragmentation chain transfer mediated polymerization of tert-butyl acrylate. *Polymer International*, 69(8), 693–701.

[18] Mengel, C., Esker, R., Meyer, H., Wegner, G. (2002). Preparation and modification ofpoly(methacrylic acid) and poly(acrylic acid) multilayers. *Langmuir*, 18(16), 6365–6372.

[19] Matyjaszewski, k., Miller, P., Shulka, N., Immaraporn, B., Gelman, A., Luokala, B., Siclovan,T., Kickelbick, G., Vallant, T., Hoffmann, H., Pakula,T. (1999) Polymers at interfaces: Using atom transfer radical polymerization in the controlled growth of homopolymers and block copolymers from silicon surfaces in the absence of untethered sacrificial initiator. *Macromolecules.* 32(26), 8716-8724.

3.7 Figures
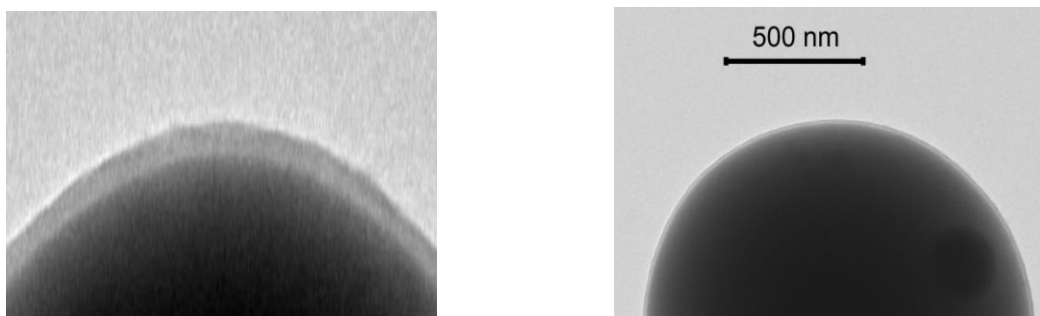
Figure 3. 1 TEM micrographs of 1.5 um acrylic acid WCX particles.
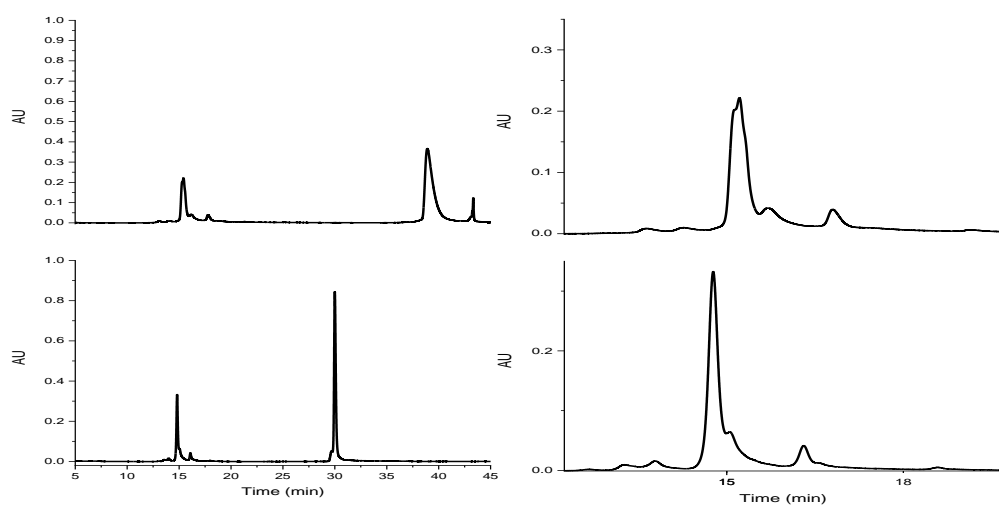
Figure 3. 2 Ides digested NIST mAb using a 5 cm lab made column (top) and a 25 cm commercial column (bottom). Both the Fab and Fc region is shown on the left, whereas a blow up of just the Fc region for both columns is shown on the right. Gradient conditions were 5-95% B in 40 minutes, 6 ug of mass was injected on the column.
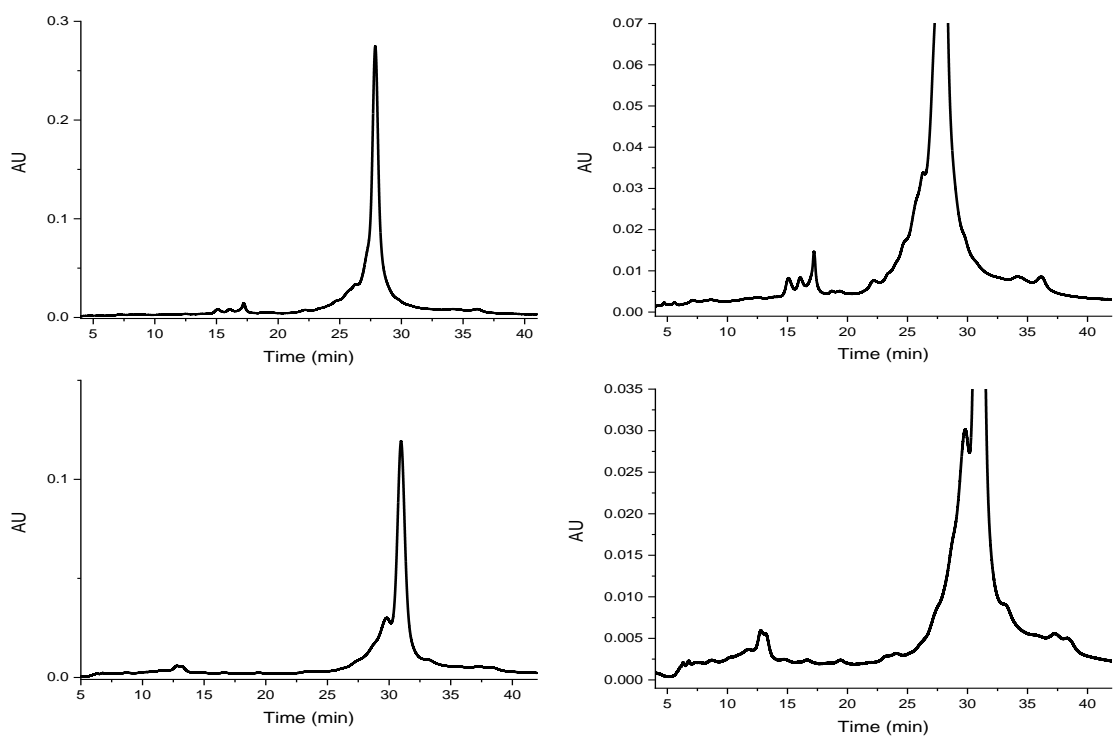
Figure 3. 3 Abbvie IgG1 mAb separation for the lab made column (top) and the commercial column (bottom). The right is a blow up version of the left. Lab made column gradient conditions were 45-85% B for 40 min. Commercial column gradient was 50-90% B in 40min6ug mass was injected.
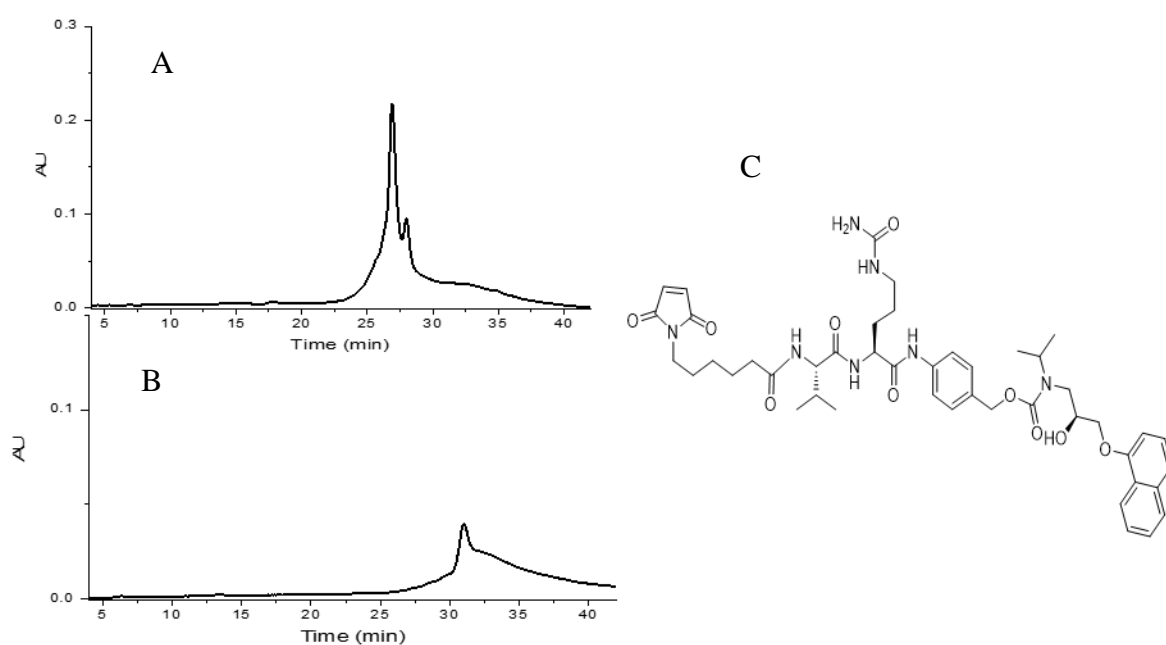
Figure 3. 4 ADC separation on the (A) the lab made column, and (B) the commercial column. The structure of the drug product and lunker used to conjugate the ADC is shown in C. Gradient conditions for the lab made column are 45-85% B in 40 minutes. The commercial column gradient was 50-90% B in 40 minutes. 6 ug mass was injected
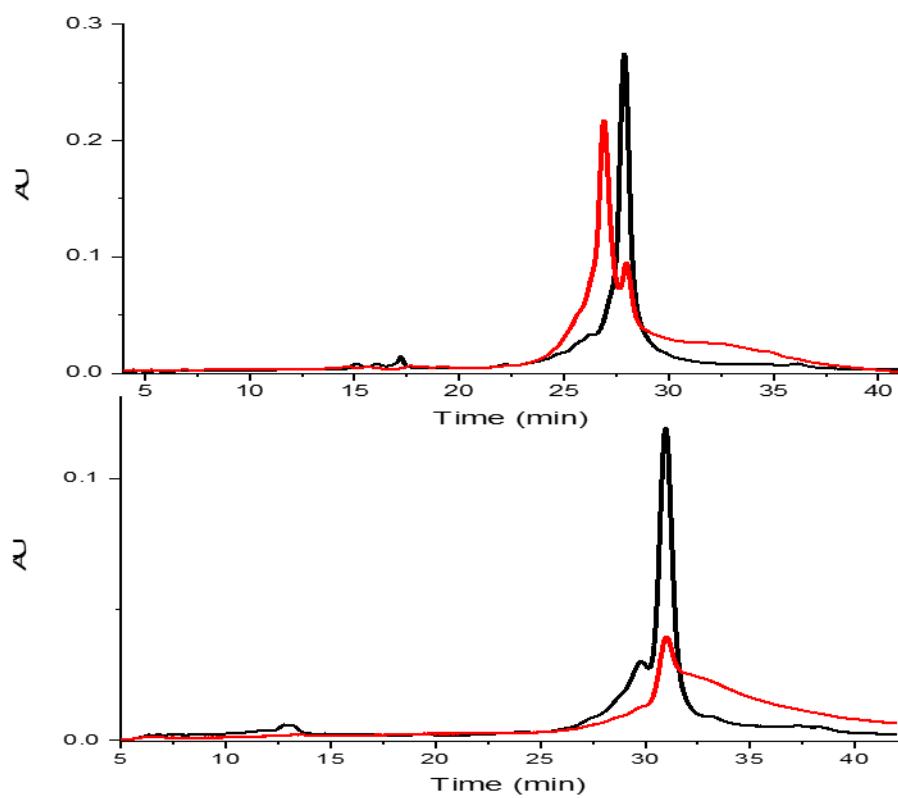
Figure 3. 5 Overlay of mAb (black trace) and ADC (red trace) separation for the lab made column (top) and commercial column (bottom). Lab made gradient conditions were 45-85% B in 40 minutes. Commercial column was 50-90% B in 40 min. 6 ug of mass was injected.

CHAPTER 4.   PROTEIN INDUCED CONFORMATIONAL CHANGE IN GLYCANS DECREASES RESOLUTION OF GLYCOPROTEINS IN HYDROPHILIC INTERACTION LIQUID CHROMATOGRAPHY

4.1   Abstract

An understanding of why hydrophilic interaction liquid chromatography (HILIC) gives higher resolution for glycans than for glycoproteins would facilitate column improvements. Separations of the glycoforms of ribonuclease B compared to its released glycans were studied using a commercial HILIC column. The findings were used to devise a new HILIC column. For the commercial column, chromatograms and van Deemter plots showed that selectivity and efficiency are comparable factors in the higher resolution of the released glycans. The higher selectivity for the released glycans was associated with more water molecules displaced per added mannose. To investigate why, three dimensional structures of the glycoprotein and the glycan were computed under chromatographic conditions. These showed that hydrogen bonding within the free glycan makes its topology more planar, which would increase contact with the bonded phase. The protein sterically blocks the hydrogen bonding. The more globular shaped glycan of the glycoprotein suggests that a thicker bonded phase might improve selectivity. This was tested by making a column with a copolymer bonded phase. The results confirmed that selectivity is increased. The findings are possibly broadly relevant to glycoprotein analysis since the structural motif involved in internal hydrogen bonding is common to N-linked glycans of human glycoproteins.

4.2   Introduction

Most human proteins, 50 to 70%, exist in a glycosylated form (1). Glycoproteins play a critical role in protein stability (2), solubility (3), cell signaling (4), immunomodulation (5), tumorigenesis (6), and protein folding (7). The carbohydrate groups alter the structure, and thus the function, of the glycoprotein (8). Considering the prevalence and importance of protein

glycosylation to human health, there is great interest in chromatographic separation of glycoproteins to assist in their identification and characterization.

HILIC resolves complex carbohydrates (9) and is the current method of choice for glycan analysis. For glycoprofiling of therapeutic monoclonal antibodies, the prevailing method is to enzymatically release the glycans. In practice, the process of isolating and derivatizing the glycan is laborious and time-consuming. The sample preparation, including digestion of the glycoprotein, extraction of the glycan, and derivatization with a suitable label such as 2-aminobenzamide (2-AB), requires many hours. This hampers the ability to monitor the glycan profile in real time during production of therapeutic monoclonal antibodies. For proteomics, the identity of the protein and the attachment site are lost in the process. Sialylation, a glycan modification that is implicated in malignant tumor development (10, 11) can be modified during the process of labelling or performing a tryptic digest to cleave the protein for glycopeptide analysis (12). These drawbacks highlight the advantages that would be provided by a rapid, top-down method of glycoprotein profiling.

HILIC has been used for separation of intact glycoproteins, albeit with lower resolution than for glycans. HILIC has been shown to give baseline separation of the five glycovariants of ribonuclease B (RNase B), which has N-linked glycosylation (13, 14). HILIC was found to be promising for glycoprofiling of therapeutic monoclonal antibodies by a middle up approach of releasing the Fc fragments, which bear the glycans (15). Despite the lower resolution, the method gives sufficient resolution of the major glycoforms to enable rapid distinction of biosimilars (16). Further, toward the goal of monitoring glycosylation of monoclonal antibodies during manufacturing, a fully automated 3D system with digestion followed by RPLC and HILIC was shown to characterize glycosylation in only 95 min (17).

Higher resolution of HILIC for glycoproteins would have significant impact. It would speed analysis time by decreasing the number of separation dimensions, lessen the reliance on mass spectrometry to simplify the instrumentation for monitoring manufacturing, and allow for additional glycoforms to be detected. To elucidate the underlying reasons why the resolution is lower for glycoproteins, this work entails a comparative study of the selectivity and efficiency of a glycoprotein versus its released glycans for the same commercial HILIC column. RNase B is used as the model glycoprotein since it is widely used as a test system for new columns, and it has N-linked glycans with many commonalities to the glycans of antibodies.

4.3 Experimental

4.3.1 Chemicals and materials

Ultrapure water was generated using a Milli-Q water purification system from Millipore (Burlington, MA) . HPLC-grade acetonitrile and isopropyl alcohol were purchased from Thermo Fisher (Waltham, MA). Nonporous silica particles of nominally 1.5 um in diameter purchased form Superior Silica (Chandlar, AZ). Concentrated nitric and acetic acid were purchased from Fischer Scientific (Pittsburg, PA). ((Chloromethyl)Phenylethyl)Dimethylchlorosilane and trimethylchlorosilane were purchased from Gelest (Morrisville, PA). N-hydroxymethylacrylamide was purchased form TCI America (Portland, OR). Copper(II) Chloride was purchased from Acros Organics (Morris Plains, NJ). (Tris(2-dimethylaminoethyl)amine (Me$_6$TREN) was purchased from Alfa Aesar (Tewksbury, MA) All other reagents, as well as proteins, were purchased from Millipore Sigma (St. Louis, MO).
2.2 Glycan Sample Preparation.

Prior to labeling, glycans were cleaved from bovine pancreatic RNase B using a modified version of the protocol described by Mann, et al. (18). For glycan cleavage, a solution was prepared containing 20 units PNGase F in 40 µL of a 50 mM PBS solution at pH 7.2. This was combined with 360 µL of a solution containing 400 µg RNase B in 50 mM PBS (pH 7.2). This solution was incubated in a water bath at 37 °C for a total of 18 hours. Residual PNGase F and deglycosylated RNase B were removed from this solution by utilizing an Amicon Ultra-0.5 mL spin filter with a 10 kDa molecular-weight cut-off cellulose membrane, spun using an Eppendorf MiniSpin microcentrifuge at 14,000·g for 20 minutes. The concentrated protein solution that did not pass through the filter was set aside for later analysis to confirm successful deglycosylation.

SPE cartridges (HILICON iSPE-HILIC) were employed to purify the glycan-containing filtrate in a process adapted from Zhang, et al. (19). Cartridges were pre-conditioned using 0.5 mL H$_2$O and 1 mL Acetonitrile (ACN), each of which was added to the cartridge and immediately removed from the sorbent using aspiration. Next, a mixture of 33 µL of the filtrate and 133 µL ACN was loaded onto the SPE cartridge. After aspirating the solvent, the cartridge was then rinsed two times with 250 µL ACN with an aspiration step after each rinse. Glycans were then eluted from the cartridge using 45 µL of a 5% ACN solution containing 100 mM ammonium acetate, with pressure applied to the head of the cartridge to assist in eluate recovery. The elution step was performed a total of three times, after which 540 µL ACN was added to the

centrifuge tube containing the purified glycan mixture, which was then placed into a -80 °C freezer for approximately one hour. After the glycan solution was completely frozen, it was uncapped and placed into a vacuum chamber for overnight lyophilization, in a process adapted from Merry, et al. (20).

Glycans were labeled with a fluorescent dye, 2-aminobenzamide (2-AB) using a protocol originally developed by Bigge, et al. (21), modified to increase sample size. A mixture of 150 µL acetic acid and 350 µL DMSO was created, with 100 µL of this mixture added to 5 mg of dried 2-AB. The solution was mixed using vortexing for approximately one minute, until the dye was completely dissolved. Finally, 6 mg of the reducing agent sodium cyanoborohydride was added to the dye mixture, which was then sonicated for five minutes until there were no visible particulates. 15 µL of this dye mixture was then added to the centrifuge tube containing the dried glycan sample, which was tightly sealed and placed into a water bath for 3 hours at 65 °C. After removing the solution from the water bath, a Waters Glycoworks HILIC 1cc SPE cartridge was used to purify the newly-labeled glycans following the protocol from the manufacturer (22). Cartridges were preconditioned with 100 µL H_2O, and 100 µL of 85/15 ACN/H_2O, with aspiration performed immediately after loading each solvent. The ACN content of the sample was brought to 80%, and the sample was then loaded onto the cartridge, followed by immediate aspiration. The cartridge was rinsed twice with 85/15 ACN/H_2O and dried using vacuum aspiration. Finally, sample was eluted using 100 µL of a 100 mM ammonium acetate solution in 5% ACN. The eluate was recovered by applying pressure to the head of the cartridge with a syringe and placed into a -80 °C freezer for approximately 30 minutes. The frozen glycan sample was then placed in a vacuum chamber for overnight lyophilization, and reconstituted in 30 µL of a solution containing 70% ACN.

4.3.2 Chromatographic Methods.

The chromatograph used in this study was a Waters Acquity I-Class UPLC instrument. An Acquity UPLC Glycoprotein Amide column with dimensions of 10 cm x 2.1 mm containing 1.7 µm particles with 300 Å pores was purchased from Waters Corporation and used for all chromatographic runs. Detection by UV absorbance was performed with a 0.5 µL detector at 280 nm. For detection by mass spectrometry, the eluent from the LC column was directed into a Thermo Ion Max ion source for analysis using a Thermo LTQ Velos linear ion trap mass

spectrometer. The electrospray voltage was set to 3.0 kV, with an inlet capillary temperature of 300°C. Nitrogen was employed as a sheath gas at a pressure of 40 psi. Data were analyzed using OriginLab OriginPro.

Prior to chromatographic analysis, glycoprotein samples were prepared in a 70% ACN diluent, containing 0.1% TFA to aid in solubility (23). All runs were performed with the thermostatted column compartment held at 30 °C, and 0.1% TFA was used as the mobile phase additive. For gradient elution, the gradient steepness was the same for glycoprotein and glycan analytes. The gradient profile for the glycoproteins was 70–55% ACN over 45 minutes, and for the free glycans was 75–60% ACN over 45 minutes. The flow rate was 100 µL/min. The injected amount was 0.3 µg/mL in all cases.

Isocratic runs used in generating the van Deemter plots, with mobile phase compositions chosen to give approximately the same retention factor for both analytes: k_{glycan}=4.4 and $k_{glycoprotein}$=4.1 for 68% and 64.5% ACN for glycan and glycoprotein, respectively. A partial loop injection method was used for all analyses, with 1 µL injected from a 10 µL sample loop. For isocratic chromatograms, the flow rate was 100 µL/min, temperature was 30 °C and 0.1% TFA was used.

4.3.3   Copolymer column.

The copolymer brush layer was made using atom transfer radical addition. Nonporous silica particles of nominally 1.5 um in diameter were calcined at 600 °C for 12 hours. This process was repeated 3 times followed by annealing at 1050 °C for 3 hours and finally rehydroxylated by refluxing in 1 M nitric acid for 24 hours. Particles were reacted with the silane initiator, ((Chloromethyl)phenylethyl)dimethylchlorosilane,and then endcapped with trimethylchlorosilane. For the polymer brush layer, 0.4 g of particles were suspended in 7.5 mL of nitrogen purged ethanol by stirring. A monomer mixture was prepared using 1.11 g of acrylamide, 1.58 g N-hydroxymethylacrylamide and 12.5 mL of nitrogen-purged water. The catalyst was prepared by mixing 40 mg $CuCl_2$, 80 ul Me_6TREN and 2.5 mL nitrogen purged water, and sonicated until dissolved. A solution of 20 mg sodium ascorbate, 2.47 mL of nitrogen-purged water, and 30 uL of 1.74 M Acetic acid was prepared. The solutions were mixed by adding the monomer mixture followed by the catalyst to the particle suspension and placed in 38 °C water bath with a nitrogen balloon. The sodium ascorbate solution was then added, and the

reaction was carried out for 1 hr. Particles were rinsed 3 times with ultrapure water, and dried in a vacuum oven. The dry thickness of the resulting polymer brush layer was found by TEM to be 7 nm. A stainless steel column (Isolation Technologies, Northbrook, IL), 2.1 mm x 50 mm, was packed with 0.25 g of reacted particles suspended in 30% ACN:H$_2$O to a pressure of 17,000 psi under sonication, as described in earlier work (24). The hydrophilic copolymer bonded phase is covered by an issued patent (25).

4.3.4   Molecular Modeling.

The structure for RNase A (ID: 1FS3) (26) was obtained from the RCSB Protein Data Bank. It was then glycosylated *in silico* and a preliminary energy-minimization step was performed using GLYCAM-Web (27) with AMBER ff12SB (28) and GLYCAM06 (29) force fields applied to the protein and carbohydrate moieties, respectively. Free glycan structures were obtained from the GLYCAM oligosaccharide libraries, and were labeled *in silico* with 2-AB using Avogadro modeling software (30). In preparation for molecular geometry optimization, glycoproteins were protonated using PROPKA (31) with pH at 2.1 to account for the presence of trifluoroacetic acid in the mobile phase (32). Each glycan and glycoprotein structure was then solvated in a 65% (v/v) acetonitrile solution using PACKMOL (33). Final geometry optimization was performed using Desmond molecular dynamics software (34), with a TIP4P water model and OPLS3e all-atom force field employed. After computing energy-minimized structures, YASARA was used to determine the van der Waals radius and radius of gyration for each molecule (35), Structures were visualized using Pymol (36) and UCSF Chimera (37).

4.4   Results and Discussion

The higher HILIC resolution for free glycans compared to intact glycoproteins is illustrated in Figure 4.1a and 4.1b. Using the same column and employing gradient elution with the same slope, the first two major peaks in the glycan sample are separated with nearly three-fold higher resolution than for the glycoprotein sample. The resolution was calculated by converting the peak FWHM to 4σ to lessen the impact from minority species eluting between the major peaks (38). An optimized gradient for the protein would be shallower since the slope of log(k) vs. percent water would be higher. An objective comparison can be made with isocratic elution, and

this is possible because the range of retention factors is narrow for these separations. Setting the retention factor to be similar for the Man5 peak, and the comparison is shown in Figure 4.1c and 4.1d. These chromatograms show that the resolution is higher for the glycans due to both narrower peaks and higher selectivity. It is interesting that the widths are so similar since one would expect the efficiency for protein separation to suffer much more from interparticle diffusion. It is also interesting that the selectivity is rather similar for the two chromatograms, whereas one might expect the large protein to obscure the small differences imparted each added mannose of the glycan. Both selectivity and efficiency are investigated.

To study efficiency, van Deemter plots for Man5 glycan and the purified Man5 variant of intact RNase B are given in Figure 4.2a. The van Deemter B term was found to be negligible in both cases, which is expected since the diffusion coefficients of the protein and the glycan are on the order of 10^{-6} cm^2/s or less, thereby contributing less than 1 μm to the plate height at the lowest flow rate studied. The C term is an order of magnitude lower for the free Man5 glycan than for its glycoprotein counterpart, 1.4±0.1 s and 13.8± 0.6 s, respectively. This is attributed to slower intra-particle diffusion, as expected for a protein analyte (39). The typical working range suggested by the column manufacturer (40) is highlighted in blue, showing the efficiency for the glycan is two to three times than that for the intact protein under these conditions. The intercept in the van Deemter plot is significantly higher for protein than for the glycan: 12.5±0.8 and 9.3±0.5, respectively. This is attributed to protein heterogeneity, which is indicated in the deconvoluted mass spectrum of Figure 4.2b. While the masses of 15,013, 15,131 and 15,124 are consistent with TFA adducts, the peaks in between are likely from proteoforms. The inset confirms this: the extracted ion chromatogram is narrower than the UV chromatogram. When corrected for the 20% contribution of heterogeneity from UV detection, as determined from the extracted ion chromatogram, the intercept becomes 8.8±0.6 um, in agreement with that for the glycan. The intercept agrees with that previously observed for the same instrument (41). Even with the heterogeneity and the much higher C term for the protein, the efficiencies differ by less than a factor of three in the middle of the operating range, giving less than a two-fold difference in peak widths.

To study selectivity, log-log plots of analyte retention factor versus mole fraction of water were prepared for each of the glycans and glycoforms. Selectivity, α, is defined as the ratio of retention factors for adjacent peaks, represented here by the Man5 and Man 6 peaks.

(4.1) $$\alpha = k_{Man6}/k_{Man5}$$

The plots in Figures 4.3a and 4.33b show that selectivity is quite different for the glycans and glycoforms, respectively, illustrating how selectivity changes with mole fraction of water. The parameters from the linear fits are summarized in Table 4.1 A comparison of selectivities can be made by choosing the same k_{Man5}, appropriately a retention factor that gives a feasible separation. The value of $k_{Man5}=4$ is used because it gives a feasible range of retention factors and is similar to that in the isocratic chromatograms of Figure 4.1. One can visually assess selectivity from the plots because the ratio corresponds to differences on the log scale. In Figure 3a for the glycans, a red box is used to show the difference between $\log(k_{Man6})$ and $\log(k_{Man5})$ for $k_{Man5}=4$. A red box is drawn in Figures 3a and 3b for the mobile phase composition where $k_{Man5}=4$, showing an obviously lower selectivity for the glycoprotein. The selectivities, indicated in the plot, are 1.44 and 1.29 for the glycans and protein glycoforms, respectively. Resolution is proportional to 1-α, therefore, the selectivity contribution 50% higher resolution for the released glycans. This is comparable to the contribution that efficiency makes to the higher resolution of the released glycans.

Table 4. 1 Slopes (absolute values) and intercepts of the data of Figure 4.3a and 4.3b, fit to Equation 4.1 for the commercial column. The difference in slopes between Man5 and Man9 is twice as large for the glycans (Δm=3.3) as for the glycoforms (Δm=1.5).

Commercial column	Man5	Man6	Man7 (avg)	Man8	Man9
Slopes (absolute values)					
Glycoprotein	27.4	27.8	28	28.7	28.9
	±0.1	±0.1	±0.1	±0.2	±0.2
Glycans	8.74	9.7	10.57	11.59	12.03
	±0.04	±0.04	±0.04	±0.04	±0.04
Intercepts					
Glycoprotein	-5.26	-5.23	-5.19	-5.22	-5.19
	±0.02	±0.03	±0.01	±0.03	±0.04
Glycans	-1.54	-1.62	-1.69	-1.78	-1.78
	±0.01	±0.01	±0.01	±0.01	±0.01

It might seem surprising that the selectivity for the glycans is only 50% higher than for the glycoproteins. With the three-fold lower slope in Figure 4.3a, along with large distance from 100% water, selectivity should be much higher for the glycans. Figures 4.3c and 4.3d provide illumination. Figure 3c shows that a three-fold lower slope does indeed give an inordinate increase in selectivity when the minimum retention factor is held constant. But this situation is not realized for the glycan separation because the high intercept is an offsetting factor. Figure 4.3d illustrates that a higher intercept gives lower selectivity when all else is the same. From Table 4.1, while the glycans have the lower slope, their intercept is more than 3 units higher than for the RNase B glycoforms, hence the advantage of the lower slope is offset by the intercept. Worse, the intercepts for the five glycans are different from one another, trending in opposite directions from HILIC, indicating that they have some reverse-phase selectivity at 100% water. The bonded phase has previously been shown to give reversed-phase retention under extremely aqueous conditions (42). For the glycans, the slight reversed-phase behavior is attributed to the benzyl group of the label, consistent with previous literature that has described an analyte-

specific balance of HILIC and RPLC-type separation mechanisms (43). The offsetting factors of slope and intercept explain why the glycoprotein separation is nearly competitive with the glycan separation.

The lower selectivity and lower efficiency for the glycoproteins exact a high price in applications because there are additional proteoforms as shoulders on the peaks. At least one extra peak is obvious for the glycoprotein in Figure 4.1d between the Man5 and Man6 peaks and between the Man6 and Man7 peaks. For increasing resolution of protein separations, much attention has been paid to improving efficiency over the past two decades with the introductions of sub-2-μm particles and superficially porous particles. Any insight that can alleviate the loss of selectivity of proteins would be just as helpful for development of columns for improving selectivity.

Soczewiński *et al*. provided a model that offers some insight from the log-log plots in Figure 3. They related the retention factor to the volume fraction of strong solvent, X_s, based on the law of mass action describing the number of strong solvent molecules, m, displaced from the surface upon adsorption of the analyte (44).

(4.2) $$log\ (k) = log(k_0) - m \cdot log(X_s)$$

The strong solvent is water in the case of HILIC. The intercept is $log(k_0)$, where k_0 is the retention factor when the mole fraction of strong solvent is unity. Although Soczewiński *et al*. based their model on normal-phase chromatography, its general application to HILIC has been affirmed (43, 45). Having the slope equal the number of water molecules displaced enables further interpretation of the data in Table 4.1.

The values of m are larger for the glycoproteins than for the glycans, as discussed earlier, and this means the protein moiety displaces about two dozen or more water molecules from the surface. It is the difference in the number of water molecule, i.e., the difference in slope imparted by each added mannose group that dictates selectivity. The differences in the slope move the lines apart. One can see from Table 4.1 that that the difference in values of m between Man5 and Man9 is more than two-fold smaller for the intact glycoprotein than for the free glycans. Not only are the slopes unfavorably higher for the glycoprotein, but the differences in slopes are unfavorably lower. Figure 4.3c had illustrated the effect of higher slope for the same Δm, now it is being emphasized that Δm is smaller for the glycoproteins. Physically, each additional mannose group on the glycoprotein displaces less water than does each additional mannose on

the glycan. This means that the protein must in some way partially shield the added mannose from interaction with the stationary phase, causing the observed decrease in selectivity for the glycoforms of the intact protein. While one might not be able to make the slope lower for the glycoprotein, one might be able to make the differences in slope higher among the glycoforms.

The means by which the protein restricts the ability of an added sugar group to displace additional water was investigated by molecular modeling. The structures of the glycan were computed for the HILIC condition of 60% acetonitrile, and these are illustrated for the Man5 case in Figures 4a and 4b. The structures reveal that the free 2-AB labeled glycan, but not the glycan of the glycoprotein, undergoes internal hydrogen bonding. The groups involved in hydrogen bonding are denoted in the inset of Figure 4a, showing that the hydrogen bonding occurs on the end opposite to where mannose groups are added. This internal hydrogen bonding necessarily gives a different three dimensional structure. The distance between the two groups involved in hydrogen bonding, which are the carbonyl of an N-acetylglucosamine and the -OH group of a mannose, is 1.7 Å for the glycan, indicative of a strong hydrogen bond, but is 6.8 Å for the glycoprotein, indicative of negligible hydrogen bonding. The distances change only slightly for the higher mannose glycans. The protein sterically blocks the approach of the hydrogen bonding pair, i.e., the mannose and N-acetylglucosamine, preventing hydrogen bond formation for the case of the glycoprotein. The same thing happens for the other glycans of RNase B.

How the hydrogen bonding affects the three dimensional structure of the glycan moiety is depicted in space-filling models of Figures 4.4c and 4.4d. Hydrogen bonding makes the free glycan structure more planar, whereas the lack of hydrogen bonding gives a more globular structure for the glycan when attached to the protein. From these structures, a reasonable explanation for how the free glycan displaces more water is that its more planar structure affords a larger area of interaction with the HILIC bonded phase. Given how few water molecules are displaced by the glycan, i.e., one water molecular per added sugar group, according to Table 4.1, its interaction with the chromatographic surface is arguably more two-dimensional than three dimensional. A thicker HILIC bonded phase might improve HILIC selectivity for glycoproteins by approaching a more three-dimensional interaction.

To test the idea that a thicker bonded phase could increase HILIC selectivity of the glycoprotein, a hydrophilic polymer brush layer of a copolymer of acrylamide and N-

hydroxymethylacrylamide was prepared on 1.5 μm nonporous silica particles, which were packed in a column having dimensions of 2.1 x 50 mm. Various copolymer growth times were performed to optimize polymer length and was characterized with TEM (figure 4.5). A controlled growth is seen between growth times of 15 , 30, and 60 minutes. The 10 minute reaction showed no visible growth and therefore was not included in the growth curve in figure 4.5. All growth times, including 10 minutes, were packed and tested with RNaseB with a gradient elution (Figure 4.6). The 10 minute growth time showed RNasaeB separation and therefore was considered a monolayer of the copolymer on the silica surface. The 10 minute separation shows increased selectivity on its own than compared to the commercial column (figure 4.1), therefore the copolymer has inherent selectivity that the commercial column does not. Compring the various growth times (figure 4.6), it can be seen that selectivity increases with reaction time. This can easily be seen by comparing the spacing between the Man5 and Man9 peaks between 10 min, 15 min, and 30 min columns. It shows that a thicker water layer results in better selectivity, up to a certain point. The selectivity difference between 30 min and 60 min does not change, indicating the optimal polymer length is reached after 30 minutes. Comparing efficiencies between the 30 and 60 min columns shows that the longer polymer length decreases efficiency. This is attributed to increased protein interaction with the stationary phase, resulting in slower protein desoprtion from the surface and lower efficiency. The 30 minute growth time of copolymer length of 7 nm was therefore used here on out because of the optimized selectivity and efficiency compared to other copolymer lengths.

Figure 4.7a shows a log-log plot of retention factor vs. mole fraction of water for the copolymer in comparison to the commercial bonded phase, showing higher selectivity. Specifically, the selectivity is increased from 1.29 to 1.37 for $k_{Man5}=4$. With resolution being proportional to $(1-\alpha)$, the resolution would be increased by 30%, with all other factors being equal.. The parameters from the linear regression are summarized in Table 4.2, showing a 30% increase in the number of water molecules displaced by the copolymer. The intercepts are the same for each of the glycoforms for the copolymer, indicating negligible reversed-phase character. The intercept is lower than for the commercial column, as one would expect for the lower phase ratio of the nonporous particles. This shifts the mobile phase composition needed to achieve $k_{man5}=4$ to be about the same as that for the released glycans, showing graphically that the resolution is approaching that for the released glycans, but is still smaller. Overall, the

observed increase in the amount of amount of displaced water per added mannose to give a larger difference in slopes among the glycoforms supports the interpretation that a thicker HILIC bonded phase gives higher area of contact between glycan and bonded phase. This improves selectivity for the glycoprotein.

Table 4. 2 Linear regression data for figure 4.7a. Slope error measurements are 0.1 for both columns.

	Man5	Man6	Man7(avg)	Man8	Man9
Slopes (absolute values)					
Copolymer	27.5	28.3	29.1	29.7	30.2
Commercial	27.4	27.8	28	28.7	28.9
Intercepts					
Copolymer	-6.50±0.04	-6.50±0.04	-6.50±0.04	-6.51±0.04	6.48±0.05
Commercial	-5.26±0.02	-5.23±0.03	-5.19±0.01	-5.22±0.04	-5.19

A comparison of the HILIC chromatogram of intact RNase B for the copolymer bonded phase and the commercial bonded phase is shown in Figure 4.7c, both under isocratic conditions. The chromatogram demonstrates that it is feasible to make a HILIC bonded phase from this selective material and obtain good resolution of intact RNase B glycoforms. The copolymer column is two-fold shorter, 5 cm, in contrast to the 10-cm length of the commercial phase. To put the two chromatograms on the same time scale, a two-fold higher retention factor was used for copolymer. The improvement in selectivity from the high retention factor is more than offset by the two-fold shorter column length. One can see this from the shorter time span of the glycoforms for the copolymer column. On the other hand, the nonporous particles significantly improve column efficiency, giving a plate height of 10 μm at the 100 μL/min flow rate (figure 4.7b), which is the same plate height as was obtained for the glycans. This further improves resolution. Interestingly, the copolymer column also minimize impurity proteoforms that caused congestion between the Man5 and Man6 peaks, indicating less selectivity for different proteoforms while having more selectivity for glycans. Whether this impacts only RNase B is not known yet. The glycoform structures are shown on the chromatogram to illustrate that there are multiple peaks for Man7 and Man8, which are expected based on the structures. These multiplets are hinted at in the chromatogram for the commercial column, and are resolved for the copolymer column, despite its shorter length. Further studies of the copolymer, with longer

column length and application to separations beyond the model protein, e.g., the IgG Fc glycoforms, are of interest.

The understanding developed here for the lower resolution of the glycoprotein compared to released glycans, while developed for bovine pancreatic RNase B, might have some general relevance to human N-glycosylated proteins, particularly to the HILIC separations of the Fc-glycans of monoclonal IgG1. The glycans of therapeutic monoclonal antibodies include the same afucosylated Man5 glycan as that of bovine RNase B. This Man5 glycan is an important impurity to characterize and control in therapeutics because it leads to unfavorably fast pharmacokinetics (46) and lower IgG stability (47). Further, the sequence involved in hydrogen bonding for RNase B, which is *asn-GlcNAc-GlcNAc-Man* followed by branching to two mannoses, is ubiquitous among human glycoproteins, and this sequence contains the two moieties that undergo hydrogen bonding in bovine RNase B. On the other hand, human glycoproteins have a high abundance of fucosylation on the first N-acetylglucosamine (GlcNAc), which might affect glycan folding differently. The results shown here for the decrease in selectivity by displacement of water by the protein moiety will likely have some relevance to the analysis of Fc glycosylation. In addition, the deglycosylated Fc fragment has a higher molecular weight than RNase A, 26 vs 12 kDa, respectively, and the results here suggest that this could give a higher slope to decrease selectivity of the HILIC separation of the Fc-glycans.

4.5 Conclusion

The basic research presented here shows that the area of contact between a glycan and an amide-type HILIC bonded phase is decreased when it is bound to a protein through N-glycosylation. The lower contact area decreases HILIC selectivity. A new bonded phase that is a thicker, designed to afford a larger contact area, is shown to improve HILIC selectivity. The conclusion is supported by log-log plots of retention factor vs. mole fraction of water, computation studies, and measurements for a polymer brush layer.

4.6 References

[1]   Apweiler, R., On the frequency of protein glycosylation, as deduced from analysis of the SWISS-PROT database. *Biochimica et Biophysica Acta (BBA) - General Subjects* 1999, *1473*, 4-8 DOI: 10.1016/s0304-4165(99)00165-8.

[2]   Mimura, Y., Church, S., Ghirlando, R., Ashton, P., Dong, S., Goodall, M., Lund, J., Jefferis, R., The influence of glycosylation on the thermal stability and effector function expression of human IgG1-Fc: properties of a series of truncated glycoforms. *Molecular immunology* 2000, *37*, 697-706.

[3]   Tams, J. W., Vind, J., Welinder, K. G., Adapting protein solubility by glycosylation. *Biochimica et Biophysica Acta (BBA) - Protein Structure and Molecular Enzymology* 1999, *1432*, 214-221 DOI: 10.1016/s0167-4838(99)00103-x.

[4]   Zhao, Y.-Y., Takahashi, M., Gu, J.-G., Miyoshi, E., Matsumoto, A., Kitazume, S., Taniguchi, N., Functional roles of N-glycans in cell signaling and cell adhesion in cancer. 2008, *99*, 1304-1310 DOI: 10.1111/j.1349-7006.2008.00839.x.

[5]   Atochina, O., Da'Dara, A. A., Walker, M., Harn, D. A., The immunomodulatory glycan LNFPIII initiates alternative activation of murine macrophagesin vivo. *Immunology* 2008, *125*, 111-121 DOI: 10.1111/j.1365-2567.2008.02826.x.

[6]   Hughes, R. C. Elsevier 1976, pp. 269-284.

[7]   Molinari, M., N-glycan structure dictates extension of protein folding or onset of disposal. 2007, *3*, 313-320 DOI: 10.1038/nchembio880.

[8]   Morell, A. G., Gregoriadis, G., Scheinberg, I. H., Hickman, J., Ashwell, G., The role of sialic acid in determining the survival of glycoproteins in the circulation. *Journal of Biological Chemistry* 1971, *246*, 1461-1467.

[9]   Alpert, A. J., Shukla, M., Shukla, A. K., Zieske, L. R., Yuen, S. W., Ferguson, M. A. J., Mehlert, A., Pauly, M., Orlando, R., Hydrophilic-interaction chromatography of complex carbohydrates. *J. Chromatogr. A* 1994, *676*, 191-202 DOI: 10.1016/0021-9673(94)00467-6.

[10   ] van Beek, W. P., Smets, L. A., Emmelot, P., Increased Sialic Acid Density in Surface Glycoprotein of Transformed and Malignant Cells—a General Phenomenon? *Cancer Research* 1973, *33*, 2913-2922.

[11   ] Stefenelli, N., Klotz, H., Engel, A., Bauer, P., Serum sialic acid in malignant tumors, bacterial infections, and chronic liver diseases. 1985, *109*, 55-59 DOI: 10.1007/bf01884255.

[12]   Yang, S., Zhang, L., Thomas, S., Hu, Y., Li, S., Cipollo, J., Zhang, H., Modification of Sialic Acids on Solid Phase: Accurate Characterization of Protein Sialylation. *Analytical Chemistry* 2017, *89*, 6330-6335 DOI: 10.1021/acs.analchem.7b01048.

[13]   Zhang, Z., Wu, Z., Wirth, M. J., Polyacrylamide brush layer for Hydrophilic Interaction Liquid Chromatography of intact glycoproteins. *J Chromatogr A* 2013, *1301*, 156-161 DOI: 10.1016/j.chroma.2013.05.076.

[14]   Matthew A. Lauber, S. A. M., Bonnie A. Alden, Pamela C. Iraneta, and Stephan M. Koza, Waters, Inc. 2015.

[15]   Periat, A., Fekete, S., Cusumano, A., Veuthey, J. L., Beck, A., Lauber, M., Guillarme, D., Potential of hydrophilic interaction chromatography for the analytical characterization of protein biopharmaceuticals. *J. Chromatogr. A* 2016, *1448*, 81-92 DOI: 10.1016/j.chroma.2016.04.056.

[16]   D'Atri, V., Fekete, S., Beck, A., Lauber, M., Guillarme, D., Hydrophilic Interaction Chromatography Hyphenated with Mass Spectrometry: A Powerful Analytical Tool for the Comparison of Originator and Biosimilar Therapeutic Monoclonal Antibodies at the Middle-up Level of Analysis. *Analytical Chemistry* 2017, *89*, 2086-2092 DOI: 10.1021/acs.analchem.6b04726.

[17]   Camperi, J., Dai, L., Guillarme, D., Stella, C., Development of a 3D-LC/MS Workflow for Fast, Automated, and Effective Characterization of Glycosylation Patterns of Biotherapeutic Products. *Analytical Chemistry* 2020, *92*, 4357-4363 DOI: 10.1021/acs.analchem.9b05193.

[18]   Mann, A. C., Self, C. H., Turner, G. A., A general method for the complete deglycosylation of a wide variety of serum glycoproteins using peptide-N-glycosidase-F. *Glycosylation & Disease* 1994, *1*, 253-261 DOI: 10.1007/bf00919333.

[19]   Zhang, Q., Li, H., Feng, X., Liu, B.-F., Liu, X., Purification of Derivatized Oligosaccharides by Solid Phase Extraction for Glycomic Analysis. *Plos One* 2014, *9*, e94232 DOI: 10.1371/journal.pone.0094232.

[20]   Merry, A. H., Neville, D. C. A., Royle, L., Matthews, B., Harvey, D. J., Dwek, R. A., Rudd, P. M., Recovery of Intact 2-Aminobenzamide-Labeled O-Glycans Released from Glycoproteins by Hydrazinolysis. *Anal. Biochem.* 2002, *304*, 91-99 DOI: 10.1006/abio.2002.5620.

[21]   Bigge, J. C., Patel, T. P., Bruce, J. A., Goulding, P. N., Charles, S. M., Parekh, R. B., Nonselective and Efficient Fluorescent Labeling of Glycans Using 2-Amino Benzamide and Anthranilic Acid. *Analytical Biochemistry* 1995, *230*, 229-238 DOI: 10.1006/abio.1995.1468.

[22]   Lauber, M. A., Koza, S. M., Fountain, K. J., Waters 2014, pp. 1-3.

[23]   Houen, G., The solubility of proteins in organic solvents. *Acta Chem Scand* 1996, *50*, 68-70 DOI: DOI 10.3891/acta.chem.scand.50-0068.

[24]   Zhang, Z. R., Wu, Z., Wirth, M. J., Polyacrylamide brush layer for hydrophilic interaction liquid chromatography of intact glycoproteins. *J. Chromatogr. A* 2013, *1301*, 156-161 DOI: 10.1016/j.chroma.2013.05.076.

[25]   Mary J. Wirth, Y. H., Zhaorui Zhang, Protein chromatography matrices with hydrophilic copolymer coatings. USA patent publ. date 2017.

[26]   Chatani, E., Hayashi, R., Moriyama, H., Ueki, T., Conformational strictness required for maximum activity and stability of bovine pancreatic ribonuclease A as revealed by crystallographic study of three Phe120 mutants at 1.4 Å resolution. *Protein Sci* 2009, *11*, 72-81 DOI: 10.1110/ps.31102.

[27]   http://glycam.org (last time accessed: March 30, 2020.

[28]   Salomon-Ferrer, R., Case, D. A., Walker, R. C., An overview of the Amber biomolecular simulation package. *Wiley Interdisciplinary Reviews: Computational Molecular Science* 2013, *3*, 198-210 DOI: 10.1002/wcms.1121.

[29]   Kirschner, K. N., Yongye, A. B., Tschampel, S. M., González-Outeiriño, J., Daniels, C. R., Foley, B. L., Woods, R. J., GLYCAM06: A generalizable biomolecular force field. Carbohydrates. *Journal of Computational Chemistry* 2008, *29*, 622-655 DOI: 10.1002/jcc.20820.

[30]   Hanwell, M. D., Curtis, D. E., Lonie, D. C., Vandermeersch, T., Zurek, E., Hutchison, G. R., Avogadro: an advanced semantic chemical editor, visualization, and analysis platform. *Journal of Cheminformatics* 2012, *4*, 17 DOI: 10.1186/1758-2946-4-17.

[31]   Olsson, M. H. M., Søndergaard, C. R., Rostkowski, M., Jensen, J. H., PROPKA3: Consistent Treatment of Internal and Surface Residues in Empirical pKa Predictions. *Journal of Chemical Theory and Computation* 2011, *7*, 525-537 DOI: 10.1021/ct100578z.

[32]   Liigand, J., Laaniste, A., Kruve, A., pH Effects on Electrospray Ionization Efficiency. *Journal of The American Society for Mass Spectrometry* 2017, *28*, 461-469 DOI: 10.1007/s13361-016-1563-1.

[33]   Martínez, L., Andrade, R., Birgin, E. G., Martínez, J. M., PACKMOL: A package for building initial configurations for molecular dynamics simulations. *Journal of Computational Chemistry* 2009, *30*, 2157-2164 DOI: 10.1002/jcc.21224.

[34]   Bowers, K. J., Chow, D. E., Xu, H., Dror, R. O., Eastwood, M. P., Gregersen, B. A., Klepeis, J. L., Kolossvary, I., Moraes, M. A., Sacerdoti, F. D., Salmon, J. K., Shan, Y., Shaw, D. E., IEEE.

[35]   Krieger, E., Vriend, G., Spronk, C., YASARA–Yet Another Scientific Artificial Reality Application. *YASARA. org* 2013, *993*.

[36]   Schrodinger, LLC, 2015.

[37]   Pettersen, E. F., Goddard, T. D., Huang, C. C., Couch, G. S., Greenblatt, D. M., Meng, E. C., Ferrin, T. E., UCSF Chimera--a visualization system for exploratory research and analysis. *J Comput Chem* 2004, *25*, 1605-1612 DOI: 10.1002/jcc.20084.

[38]   Kawabe, T., Tomitsuka, T., Kajiro, T., Kishi, N., Toyo'Oka, T., Ternary isocratic mobile phase optimization utilizing resolution Design Space based on retention time and peak

width modeling. *J. Chromatogr. A* 2013, *1273*, 95-104 DOI: 10.1016/j.chroma.2012.11.082.

[39]   Gritti, F., Guiochon, G., Mass transfer equation for proteins in very high-pressure liquid chromatography. *Analytical Chemistry* 2009, *81*, 2723-2736.

[40]   Koza, S. M., Lauber, M. A., Fountain, K. J., McCall, S., Bharadjwaj, R., Fournier, J., Chambers, E. E., Morris, M. F., Brousmiche, D. W., Iraneta, P. C., McCarthy, S. M., Birdsall, R. E., Yu, Y. Q., Waters Corporation 2016.

[41]   Wu, N. J., Liu, Y. S., Lee, M. L., Sub-2 mu m porous and nonporous particles for fast separation in reversed-phase high performance liquid chromatography. *J. Chromatogr. A* 2006, *1131*, 142-150 DOI: 10.1016/j.chroma.2006.07.042.

[42]   Ibrahim, M. E. A., Liu, Y., Lucy, C. A., A simple graphical representation of selectivity in hydrophilic interaction liquid chromatography. *J. Chromatogr. A* 2012, *1260*, 126-131.

[43]   Jin, G., Guo, Z., Zhang, F., Xue, X., Jin, Y., Liang, X., Study on the retention equation in hydrophilic interaction liquid chromatography. 2008, *76*, 522-527 DOI: 10.1016/j.talanta.2008.03.042.

[44]   Soczewinski, E., Waksmundzki, A., Soczewinski, E., Suprynowicz, Z., Ewell, R. H., Harrison, J. M., Berg, L., Pimentel, G. C., McClellan, A. L., Hydrogen Bond, T., Francisco, S., Solvent Composition Effects in Thin-Layer Chromatography Systems of the Type Silica Gel-Electron Donor Solvent. *J. Oscik, Bull. Acad. Pol. Sci., Ser. Sci. Chim* 1968, *5*, 7-7.

[45]   Wang, P. G., He, W., Hydrophilic interaction liquid chromatography (HILIC) and advanced applications. Taylor & Francis, Boca Raton 2011.

[46]   Boune, S., Hu, P. S., Epstein, A. L., Khawli, L. A., Principles of N-Linked Glycosylation Variations of IgG-Based Therapeutics: Pharmacokinetic and Functional Considerations. *Antibodies* 2020, *9*, 20 DOI: 10.3390/antib9020022.

[47]   Fang, J., Richardson, J., Du, Z. M., Zhang, Z. Q., Effect of Fc-Glycan Structure on the Conformational Stability of IgG Revealed by Hydrogen/Deuterium Exchange and Limited Proteolysis. *Biochemistry* 2016, *55*, 860-868 DOI: 10.1021/acs.biochem.5b01323.
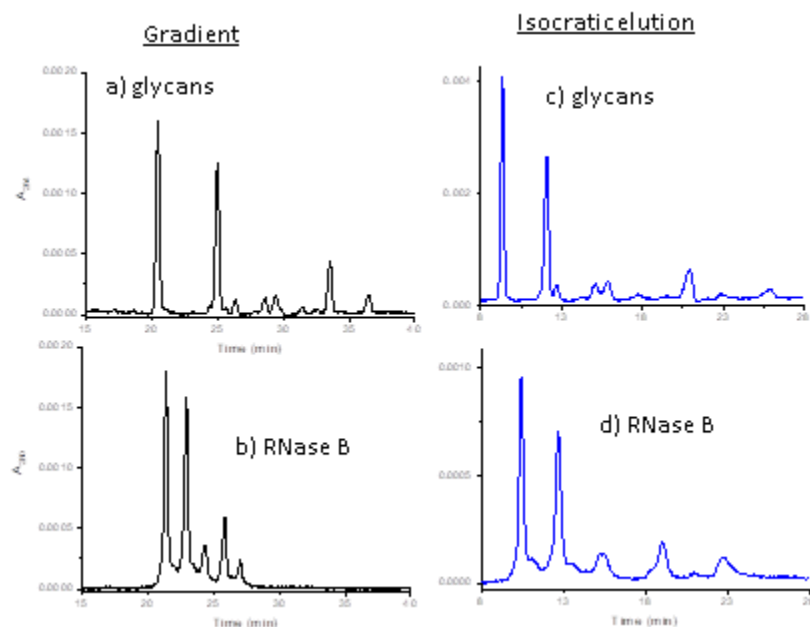
Figure 4. 1HILIC chromatograms of the a) free glycans released from RNase B and b) the glycoforms of intact RNase B, both with gradient elution. Gradient conditions: 75 – 60 % B (glycans) and 70 – 55% B (protein) over 30 minutes. HILIC chromatograms with isocratic elution chromatograms for c) the released glycans using 68% acetonitrile, and b) the glycoforms of intact RNase B using 64.5% acetonitrile. For all chromatograms, the flow rate was 100 μL/min.
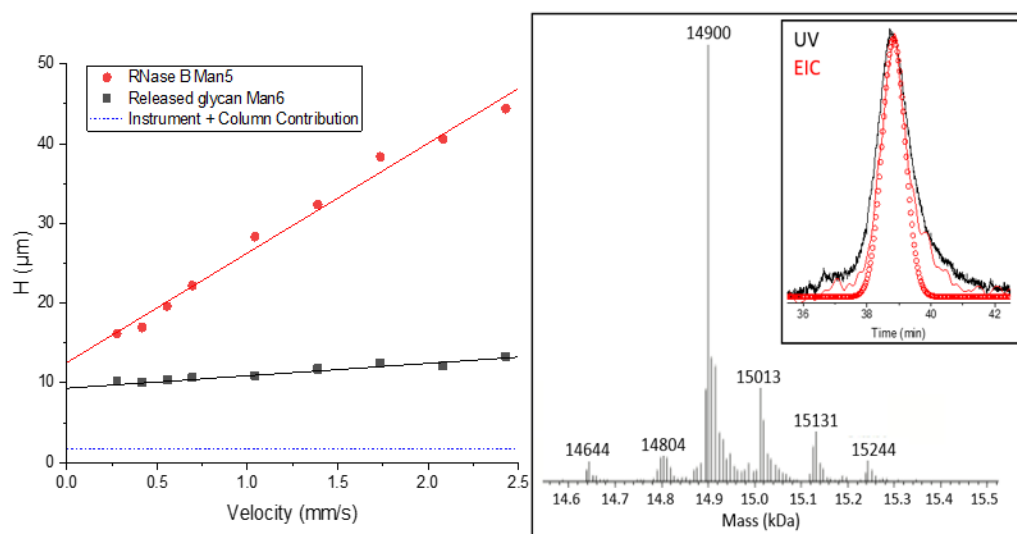
Figure 4. 2 a) The van Deemter plots for isocratic elution of a free Man5 glycan (■) and the corresponding glycoprotein (●), along with lines from least-squares fitting. The dashed line is the contribution to the plate height from the instrument plus column, as measured for the corresponding unretained peaks. b) The deconvoluted mass spectrum for the RNase B peak with its Man5 glycoform after purification through fraction collection. The inset compares the UV chromatogram (black trace) with the extracted ion chromatogram (red trace), which was obtained for largest peak in the mass spectrum.
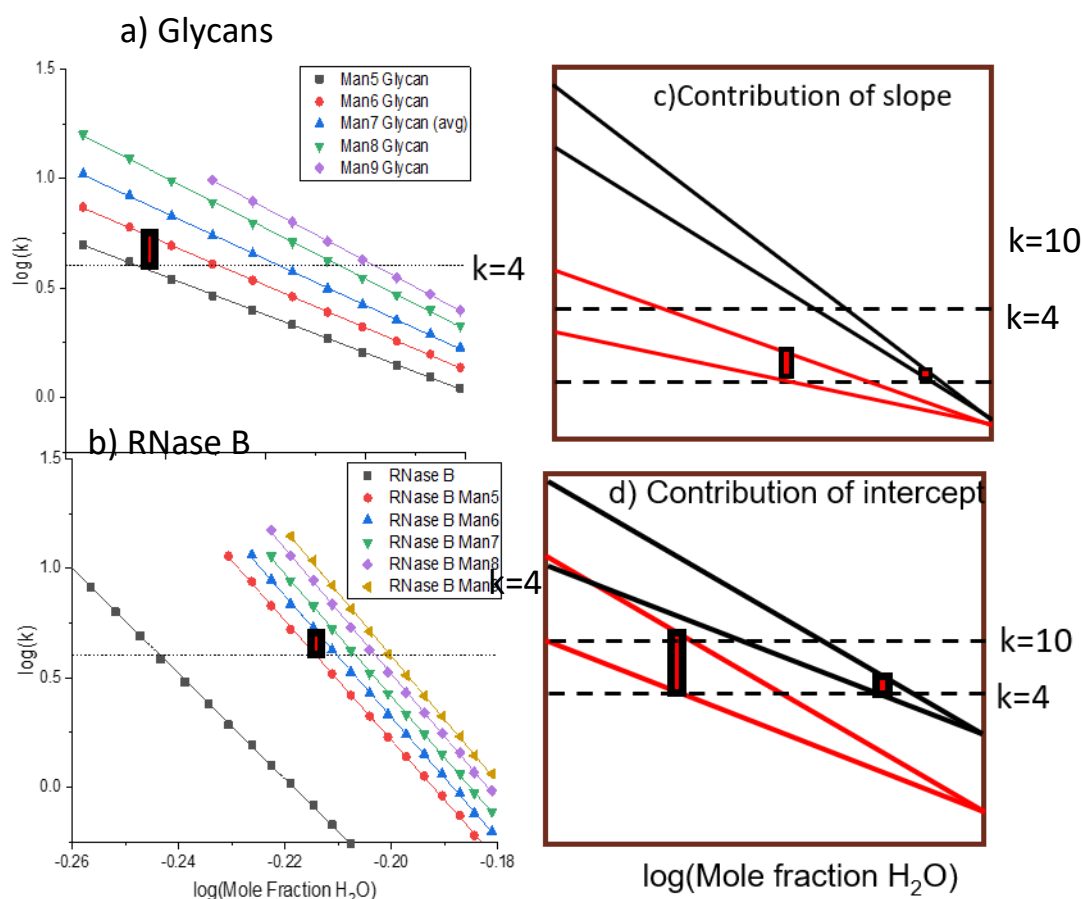
Figure 4. 3. a,b) Log-log plots of experimental values from measurements of retention vs. mole fraction of water for free glycans compared to intact glycoforms of RNase B. The horizontal dashed line corresponds to k=4. The selectivities, where α=kMan6/kMan5, are 1.44 and 1.29 for the glycans and glycoforms, respectively, when kMan5=4. The higher selectivity for the glycans is depicted by the red box connecting the traces for the Man5 and Man6 glycans when k=4 for the MAN5 glycan. c) A synthetic plot illustrates the contribution of the slope to selectivity.. d) A synthetic plot illitrates the contribution of the intercept to selectivity.
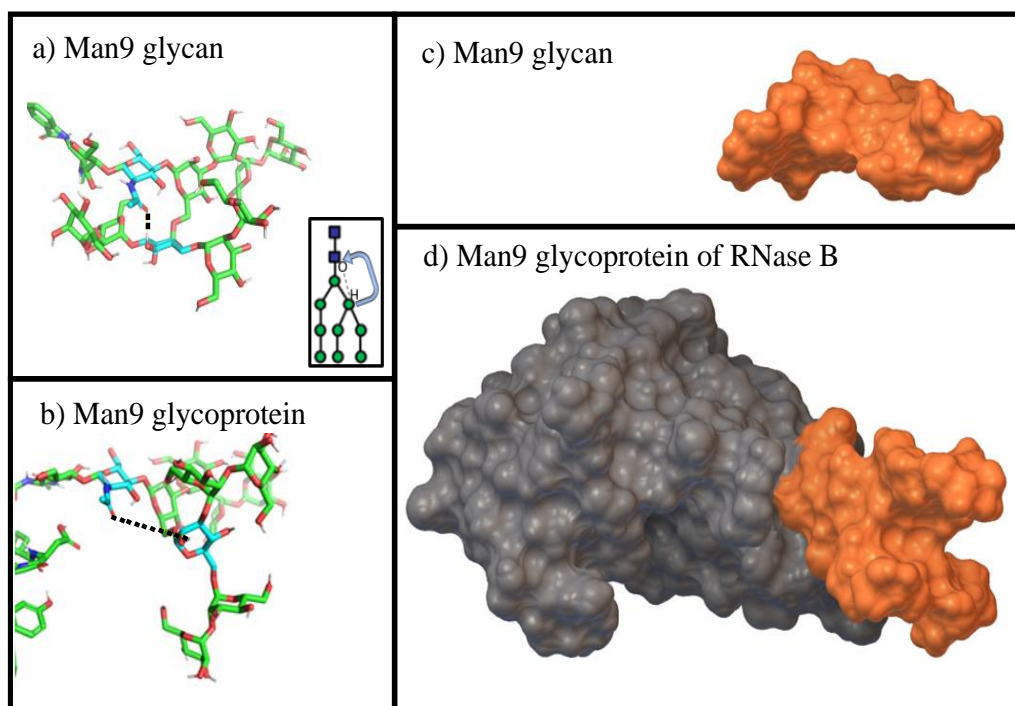
Figure 4 4. Energy-minimized structures of the glycan moiety in 60% acetonitrile/water for a) the AB-2 labeled Man9 glycan, using a black dashed line to denote intramolecular hydrogen bonding with a distance of 1.8 Å, and b) the RNase-linked Man 9 glycan, noting the same two groups as in panel a are now 6.4 Å apart. The inset in panel a shows the abbreviated glycan depiction to indicate which sugars are involved in the intramolecular hydrogen bonding. Space-filling models of c) the 2-AB labeled Man 9 glycan and d) RNase B with its the Man9 moiety rendered in the same orange color.

10 Min- No visible growth

100 nm

15 min

30 min

60 min
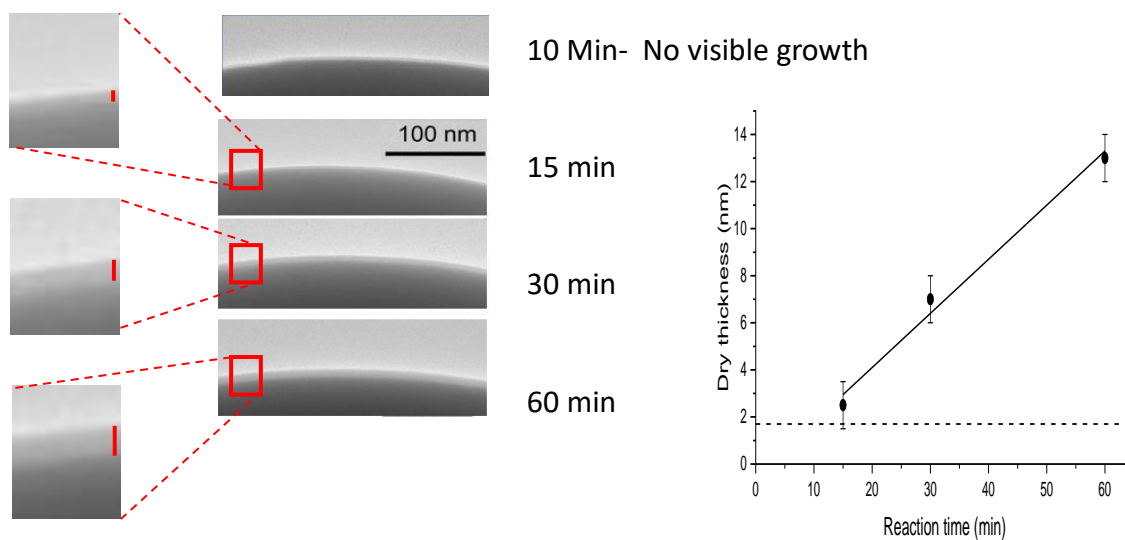
Figure 4. 5 Transmission electron micrographs as a function of copolymer reaction time. 10 minute reaction showed no visible copolymer growth using TEM and was not included in the growth curve.
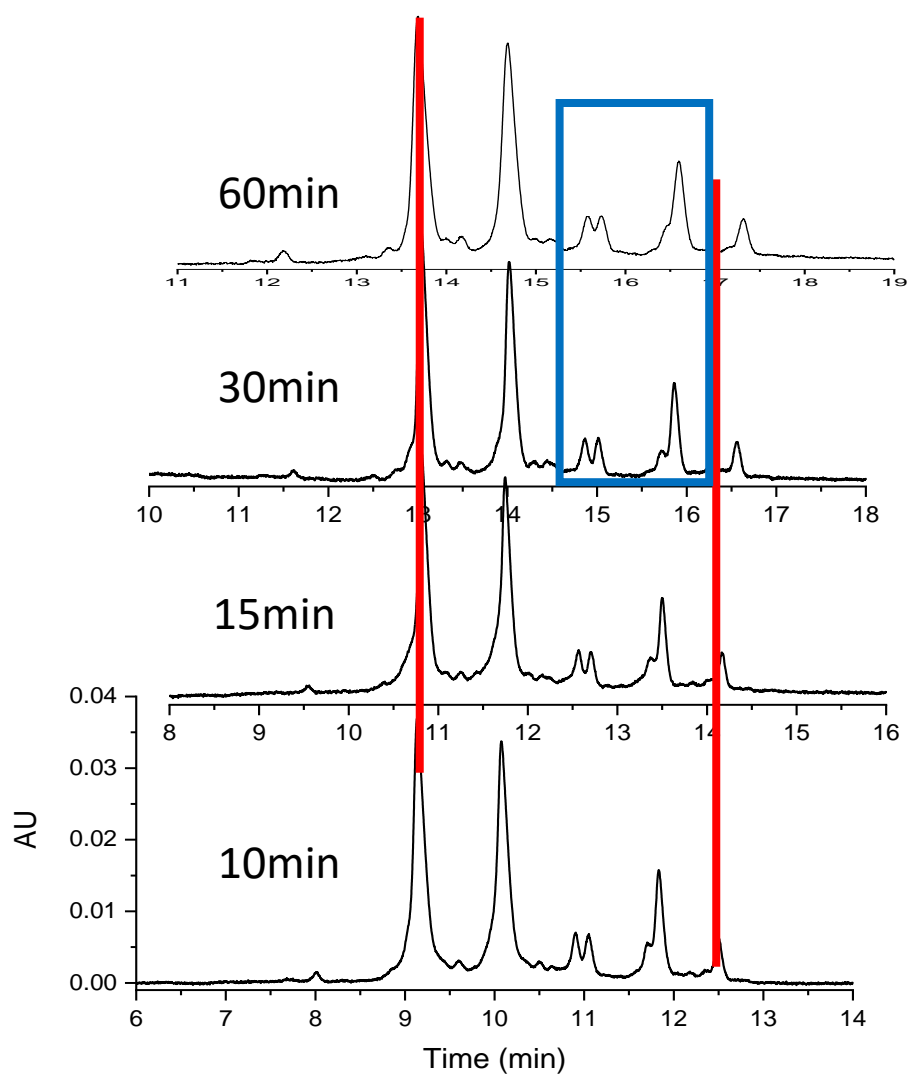
Figure 4. 6 RNaseB separation using 5 cm copolymer columns of different growth times. Man5 peak is lined up between all chromatograms. Gradient conditions were 75-65% B in 20 minutes. Red bars are used to help show improvement in selectivity and depict the distance between Man5 and Man9 for the 10 min column. Blue box is to help highlight the efficiency difference between the 30 and 60 minute chromatograms.

a)

copolymer

commercial

b)

c)

RNaseB, copolymer, isocratic
L=5 cm, k_{Man5}=8
RNase B, commercial, isocratic
L=10 cm, k_{Man5}=4
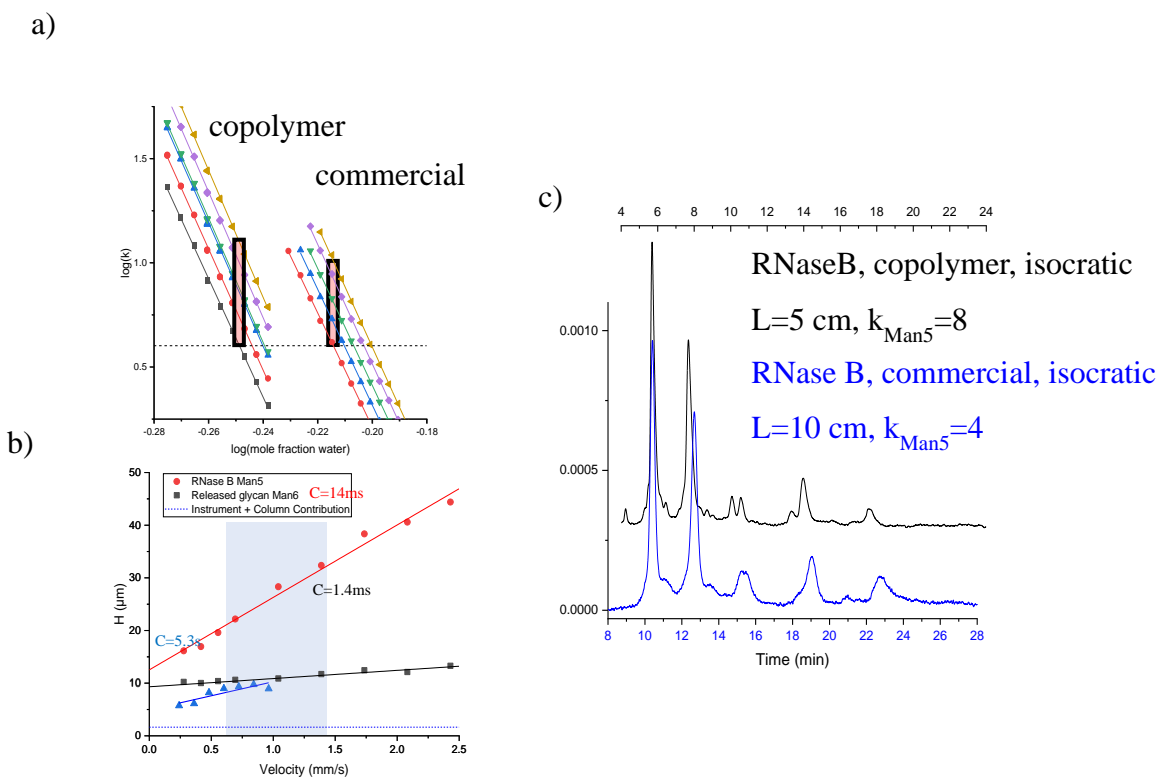
Figure 4. 7 . a) Log-log plot of retention factor vs. mole fraction of water for the RNase B separation by the copolymer, in comparison of that for the commercial column. The red boxes illustrate the higher selectivity of the copolymer for the Man5 and Man 6 glycans when k_{Man5}=4. b) Van Deemter plots comparing the commercial column glycoprotein separation (red line), the commercial column free glycan separation (black line) and the copolymer glycoprotein separation (blue line). Blue dash line represents instrument contribution and the gray shaded region represents the working range of the waters column. c) representative isocratic separations of RNaseB for the commercial column and the copolymer column. k value for Man5 were adjusted for elution over similar time spans.

CHAPTER 5. IMPROVED FC GLYCAN CHARACTERIZATION USING NEW HYDROPHILIC INTERACTION CHROMATOGRAPHY STATIONARY PHASE

5.1 Abstract

Glycan characterization is an important critical quality attribute as determined by the FDA. Glycoprotein analysis using hydrophilic interaction liquid chromatography (HILIC) is an ideal method for characterization because of its fast analysis time compared to glycan analysis. A novel HILIC stationary phase is used for the separation for monoclonal antibody FC glycoprotein characterization showing greater resolution than a commercial column. Three mAbs were used to compare the new bonded phase and glycan identification was done using inline LC-MS. Temperature optimization showed that the lab made column showed highest resolution at lower temperatures (~50 C) will maintaining higher percent recovery compared to higher temperatures. For all three IgG1s, the lab made column resolved more glycoforms than the leading commercial column, indicating that the thicker bonded phase does improve mAb separations. Glycoforms not separated in the commercial column are resolved and identified in the lab made column including 28 glycoforms in the highly complex NIST mAb.

5.2 Introduction

Therapeutic mAbs have large amounts of heterogeneity caused by modifications occurring during manufacturing, processing, and storage. Glycosylation variants are one such source of heterogeneity that need to be characterized and controlled because they can impact the mAb's immunogenicity, pharmacokinetics and biological activities. (1,2). Current glycan identification methods are typically lengthy and laborious processes resulting in glycan cleavage and subsequent labeling with a fluorescent label like 2-aminobenzamide before separation using electrophoresis or hydrophilic liquid interaction chromatography. (3-5) This long process usually takes around 14 hours from start to finish, and does not allow for real time glycan characterization of the antibody while being produced in the bioreactor.

There have been advancements in decreasing this analysis time including a recent method cleaving glycans in parallel with glycan labeling and recovery by solid phase extraction followed

by HILIC-MS (6). This method still requires multiple handling steps and all protein information is lost after cleaving the glycan.

A HILIC separation of glycoproteins without releasing the glycans would result in faster analysis time and easier real time glycan characterization. A middle up approach of analysis involving cleaving of mAb subunits with Ides enzyme and analyzing the Fc/2 fragments for glycosylation is an intriguing approach. This concept has been demonstrated (7,8) and Figure 5.1 depicts the workflow which includes Ides digestion (30 min recommended) followed by DTT reduction (10 min) to reduce the Fab portions interaction with the bonded phase. No UV labeling step would be required because of the UV active Fc portion of the mAb. This allowed for fast analysis time, but column performance showed insufficient resolution of glycoforms.

Glycoproteins separation via HILIC has been shown to have lower resolution than that of released glycans. Recently we demonstrated that the lower resolution comes from a decrease in glycan interaction for the glycoprotein than for a released glycan, resulting in lower selectivity along with lower efficiency because of the larger analyte size (9). We also demonstrated that introducing a thicker water layer improves glycoprotein resolution to be more comparable to that of a released glycan separation. This was done using a model protein (RNaseB) but it would be reasonable that this could apply to Fc/2 portions of mAbs.

In this work, we utilize this new bonded phase for the analysis of mAb Fc/2 fragments via Ides digestion and DTT reduction. HILIC solvents allow for identification of glycoforms using mass spectrometry, and therefore LC-MS was utilized for glycan identification and UV relative quantifications. The NIST IgG1 mAb and two IgG1s provided by Genentech and AbbVie were used to compare the new lab made column to a leading commercial column.

5.3 Experimental

5.3.1 Chemicals and materials

SiO_2 nanoparticles (1.5um in diameter) were purchased from Superior Silica. (Chandlar, AZ). Acrylamide and L-sodium ascorbate (98%) were purchased from Sigma-Aldrich (St. Louis, MO). HMAM was purchased from TCI chemicals (Portland,OR) Stainless steel tubings, ferrules and internal nuts were purchased from Valco Instruments (Houston, TX). Stainless steel columns, frits, and end caps were purchased from Idex (Oak Harbor, WA). 2-

(chloromethylphenylethyldimethyl) chlorosilane and trimethylchlorosilane were purchased from Gelest (Morrisville, PA). Copper(II) Chloride (99%) was purchased from Acros Organics (Morris Plains, NJ). Tris (2-dimethylaminoethyl) amine (Me$_6$TREN) was purchased from Alfa Aesar (Tewksbury,MA). Acetonitrile, ethanol, methanol, and 17.4 M acetic acid,. Pierce trifluoroacetic acid (TFA) LC-MS grade, Dithiothreitol (DTT) were purchased from ThermoFischer Scientific (Pittsburg, PA) Carboxypeptidase B and digestion buffer were purchased from G-Biosciences (St. Louis, MO) Tris base was purchased from Avantor (Radnor, PA). FabRICATOR was purchased from Genovis (Cambridge, MA) Millipore water (18.2 OHMS) was provided in house by (Burlington, MA). NIST IgG1 reference standard was purchased form the National Institute of Standards and Technologies (NIST) (Gaithersburg, MD). A commercial IgG1 was provided by Genentech (South San Francisco, CA) as well as one from AbbVie (Lake wood, IL)

A Waters HILIC Glycoprotein 10 cm 300 Å column was used to compare with the lab made column. All separations were performed on a Waters I class. An Agilent 6230B TOF instrument was used for mass spectrometry analysis.

5.3.2 Stationary phase preparation

1.5 um in diameter silica particles were heat treated at 600 °C three times for 12 hours each rinsing with 1:1 water and ethanol between each treatment. Following the third heat treatment, the particles were heated to 1050 °C for 3 hours. Particles were then rehydroxylated by refluxing in 1.5 M nitric acid for 16 hours. Particles were then rinsed with water until neutral pH, and dried in a vacuum oven. The rehydroxylated particles were then suspended in dry toluene containing 2% (v/v) chloromethylphenylethyldimethyl chlorosilane and 0.1% (v/v) butylamine. Particles were refluxed under nitrogen for 3 hours. After 3 hours, trimethylchlorosilane 2% (v//v) was added without cooling down the system and was refluxed for 3 hours. Particles were then rinsed in toluene two times and the last rinse with ethanol before vacuum drying.

SI-AGET ATRP was performed on the silicas surface as described previously. In short, 0.54 grams of initiated particles were suspended under nitrogen in 9.75 mL ethanol. 1.44 g acrylamide and 2.04 g of N-hydroxymethyl acrylamide were dissolved in 16.25 mL Millipore water and added to the particle suspension. 0.052 g CuCl$_2$, 104 uL of Me$_6$TREN, and 3.25 mL

water were sonicated together and added to the particle suspension. Nitrogen balloon was added and solution was placed in 38 °C water bath. After 10 min, 0.026 g sodium ascorbate was mixed with 3.21 mL water. Then 33.7 uL of 1.74 M acetic acid was added to the sodium ascorbate solution and then injected into the particle suspension. Reaction ran for 30min, and solution was rinsed three times with water

0.52 g of particles were suspended in 2.5 mL of water which was then packed into a stainless steel column (10.0 cm x 2.1 mm) (insert packing pump instrument) using 30% acetonitrile/ 70% water packing solution under sonication as described in previous work (source). Once the column was fully packed, a final packing solvent of 85% ACN / 15% water solution was used under sonication for 5 min. The hydrophilic copolymer bonded phase is covered by an issued patent (source).

5.3.3 Sample preparation

All mAbs were prepared in the following manor. 200 ug of mAb was diluted with 130 uL of 50 mM Tris base pH 7.5 adjusted with HCL. Then 3.2 uL of 66.67 units/uL fabRICATOR (213 units) were added along with 3.2 uL of 1 ug/uL carboxypeptidase B solution. This was then incubated at 37°C for 30 min. Then 7.7 mg of DTT were dissolved in 160 uL 50 mM Tris Base pH 7.5 and 90 uL were added to the mAb digestion and incubated for 15 min. The digestion buffer was then placed in a 15,000 Da spin filter and diluted to 500 uL with water and spun down at 14,000 gs for 5 min. The digestion was then resuspended with water to 500 uL and spun down at 14,000 gs for 10 min. The solution was then suspended in the starting gradient concentration at the indicated mass.

5.3.4 Chromatographic conditions

A Waters I class was used in all separations equipped with a low dispersion analytical flow cell with a 5 uL injection loop. Injection volumes were 1.0 uL. Solvent A was 0.1 % TFA in water and solvent B was 0.1 % TFA in ACN. Flow rates were 0.1 mL/min with a detection wavelength of 210 nm. Weak wash was 75% ACN/ 25% water and the strong wash was 50% methanol/ 50% water. All other conditions will be indicated in the relevant sections.

5.3.5   Mass spectrometry conditions

An Agilent TOF 6230B instrument was used for LC-MS analysis. For MS analysis, 0.8 ug of mAb was injected. Gas temperature 275C, drying gas 8 L/min, nebulizer 45 psi, 4000 V, Fragmentor 100V, skimmer 60V, Oct RF Vpp 750V. Mass Hunter was used for identification with manual deconvolution.

5.4   Results and discussion

5.4.1   FC glycoprotein separation

Previous work has shown that a new, thicker bonded phase results in better resolution of glycoforms for ribonuclease B (9). Using this new bonded phase, the characterization of NIST IgG1, and two commercial IgG1 provided by Genentech and AbbVie were compared to a leading commercial column. A schematic of the sample preparation used for the mAbs is shown in figure 5.1. IDES digestion using the fabRICATOR enzyme was used to cleave just below the hinge region separating the mAb into the Fab and Fc/2 fragments. It has been shown that glycoprotein variants like C-terminal lysine residues can be retained on a HILIC column (10) , therefore to reduce the complexity of the chromatogram, carboxypeptidase B was used to cleave C-terminal lysine. DTT reduction was then used to further break down the Fab fragment resulting in elution before the Fc portion and allowing for a more efficient separation do to the Fc portion no longer interacting with the retained Fab. The total sample time preparation from start to finish takes only 60 min, which is much faster than the typical 14 hours needed for cleaved glycan analysis (3-5).

Using this sample preparation method, the separation of the NIST IgG1, Genentech IgG1, and AbbVie IgG1 was compared using the lab made column and a commercial column using a 10 % gradient over 20 min.

Figure 5.2, 5.3, and 5.4 shows a comparison of the lab made column and commercial column for the separation of NIST IgG1, Genentech IgG1, and AbbVie IgG1, respectively. Comparing NIST IgG1 separations (Figure 5.2), it can be see that the lab made column is able to resolve a higher number of glycoforms than the commercial column The lab made column is able to resolve 21 different glycoform peaks compared to 15 for the commercial column where

many of the glycoforms overlap one another. This can clearly be seen by comparing the elution of the later eluting glycoforms species.

Comparing Genentech IgG1 separations (figure 5.3), it again can be seen that the lab made column provides higher resolution than the commercial column. Two early eluting peaks are seen before the main glycoform for the lab made column compared to one for the commercial column. A fully resolved peak is also seen after the main glycoform in the lab made column compared to a shoulder in the commercial column. This is later identified as the mannose 5 glycoform, which decreases the efficacy of the drug and therefore is important to characterize during the manufacturing process (11).

The AbbVie mAb comparison (figure 5.4) is more of the same with higher resolution for the lab made column. Two extra glycoforms elute later in the chromatogram that are not present in the commercial column. This along with two shoulders that begin to form right before and after the major glycoform. The improvement in resolution is not as stark as for the Genentech and NIST mAb separation, most likely because it is a less complex sample allowing for an easier separation.

5.4.2   Mass spectrometry identification of glycoforms

LC-MS was performed using the lab made column for glycoprotein identification. Double the mass was injected compared to the early chromatograms to allow for higher MS signal to aid in identification. Figure 5.5 shows the total ion chromatograms for both the AbbVie mAb and Genentech mAb separation and are labeled with the glycoproteins identified. Interestingly the mannose 5 peak, which can lead to negative side effects (12), is pulled completely away from the G0F glycoform and even begins separating out the G1 glycoform in the Genentech mAb, but is not as resolved for the separation of the AbbVie IgG1. This suggests that the orientation of the glycan is different between both mAbs resulting in more, or less interaction with the bonded phase.

Released glycan studies have shown the NIST mAb contains 35 different glycans (13). The lab made column was able to identify 28 distinct glycoforms (figure 5.6). You would expect released glycan studies to be able to identify more glycans because of less overlap decreasing ionization efficiency. The identification of 28 glycoforms and separation of 21 peaks shows the improved resolution compared to the lab made column which only separates 15 peaks.

5.5   Conclusion

A lab made, polymer shell HILIC column was shown to have higher resolution than a leading commercial column in the separation of three IgG1 mAbs. The higher resolution allowed for the greater resolution of harmful glycoforms, like mannose 5, to allow for more accurate characterization. In the separation of a highly complex NIST mAb IgG1, 28 different glycoforms were identified using mass spectrometry.

5.6   References

[1]   Arnold, J. N.; Wormald, M. R.; Sim, R. B.; Rudd, P. M.; Dwek, R. A., The Impact of Glycosylation on the Biological Function and Structure of Human Immunoglobulins. *Annual Review of Immunology* **2007,** *25* (1), 21-50

[2]   Higel, F.; Seidl, A.; Sörgel, F.; Friess, W., N-glycosylation heterogeneity and the influence on structure, function and pharmacokinetics of monoclonal antibodies and Fc fusion proteins. *European Journal of Pharmaceutics and Biopharmaceutics* **2016,** *100*, 94-100.

[3]   Hooker, A. D.; James, D. C., Analysis of glycoprotein heterogeneity by capillary electrophoresis and mass spectrometry. *Molecular Biotechnology 14* (3), 241-249.

[4]   Melmer, M.; Stangler, T.; Schiefermeier, M.; Brunner, W.; Toll, H.; Rupprechter, A.; Lindner, W.; Premstaller, A., HILIC analysis of fluorescence-labeled N-glycans from recombinant biopharmaceuticals. *Anal Bioanal Chem* **2010,** *398* (2), 905-14.

[5]   Gennaro, L. A.; Salas-Solano, O.; Ma, S., Capillary electrophoresis–mass spectrometry as a characterization tool for therapeutic proteins. *Analytical Biochemistry* **2006,** *355* (2), 249-258

[6]   Lauber, M. A.; Yu, Y. Q.; Brousmiche, D. W.; Hua, Z. M.; Koza, S. M.; Magnelli, P.; Guthrie, E.; Taron, C. H.; Fountain, K. J., Rapid Preparation of Released N-Glycans for HILIC Analysis Using a Labeling Reagent that Facilitates Sensitive Fluorescence and ESI-MS Detection. Analytical Chemistry 2015, 87 (10), 5401-5409.

[7]   Bobály, B., D'Atri, V., Beck, A., Guillarme, D., & Fekete, S. (2017). Analysis of recombinant monoclonal antibodies in hydrophilic interaction chromatography: A generic method development approach. Journal of Pharmaceutical and Biomedical Analysis, 145, 24–32.

[8]   Periat, A.; Fekete, S.; Cusumano, A.; Veuthey, J. L.; Beck, A.; Lauber, M.; Guillarme, D., Potential of hydrophilic interaction chromatography for the analytical characterization of protein biopharmaceuticals. J Chromatogr A 2016, 1448, 81-92.

[9]   Bupp,C., Schwartz, C., Wei, B., Wirth, M., (2021) Protein-induced Conformational Change in Glycan Decreases Resolution of Glycoprotein in Hydrophilic Interaction Liquid Chromatography. *Journal of Separation Science.* 44(8), 1581-1591.

[10] D'Atri, V., Fekete, S., Beck, A., Lauber, M., Guillarme, D. (2017) Hydrophilic Interaction Chromatography Hyphenated with Mass Spectrometry: A Powerful Analytical Tool for the Comparison of Originator and Biosimilar Therapeutic Monoclonal Antibodies at the Middle-up Level of Analysis. *Analytical Chemistry.* 89(3): 2086-2092

[11] Goetze, A., Liu, Y., Zhang, Z., Shah, B., Lee, E., Bondarenko, P., Flynn, G. (2011) High-mannose glycans on the Fc region of therapeutic IgG antibodies increase serum clearance in humans. *Glycobiology*. 21(7) 949-59.

[12] Yu, M., Brown D., Reed, C., Chung, S., Lutman, J., Stefanich, E., Wong, A., Stephan, JP., Bayer, R. (2012) Production, characterization and pharmacokinetic properties of antibodies with N-linked Mannose-5 glycans. *mAbs*, 4(4), 475-487.

[13] Hilliard, M., Alley, W., McManus, C., Yu, Y., Hallinan, S., Gebler, J., Rudd, P. (2017) Glycan characterization of the NIST RM monoclonal antibody using a total analytical solution: From sample preparation to data analysis. *MAbs*. 9(8): 1349-1359.
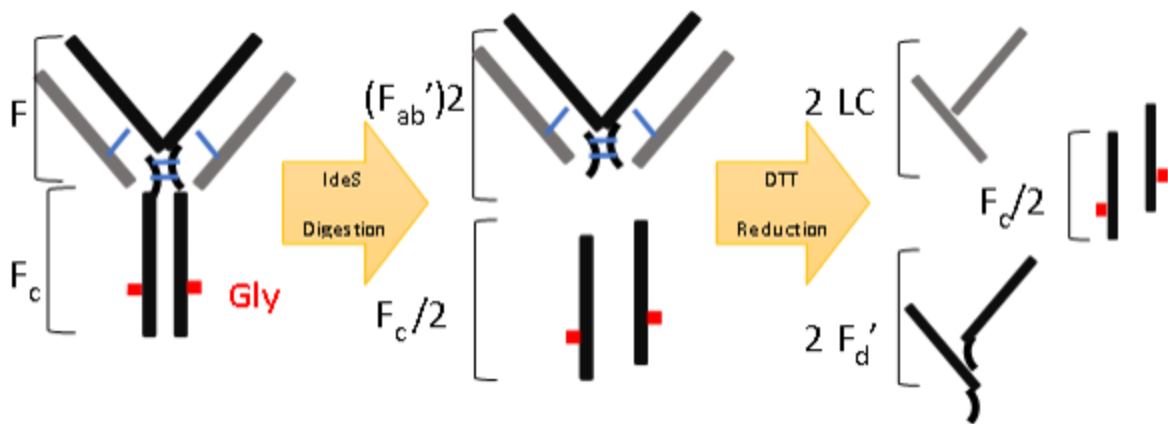
5.7   Figures

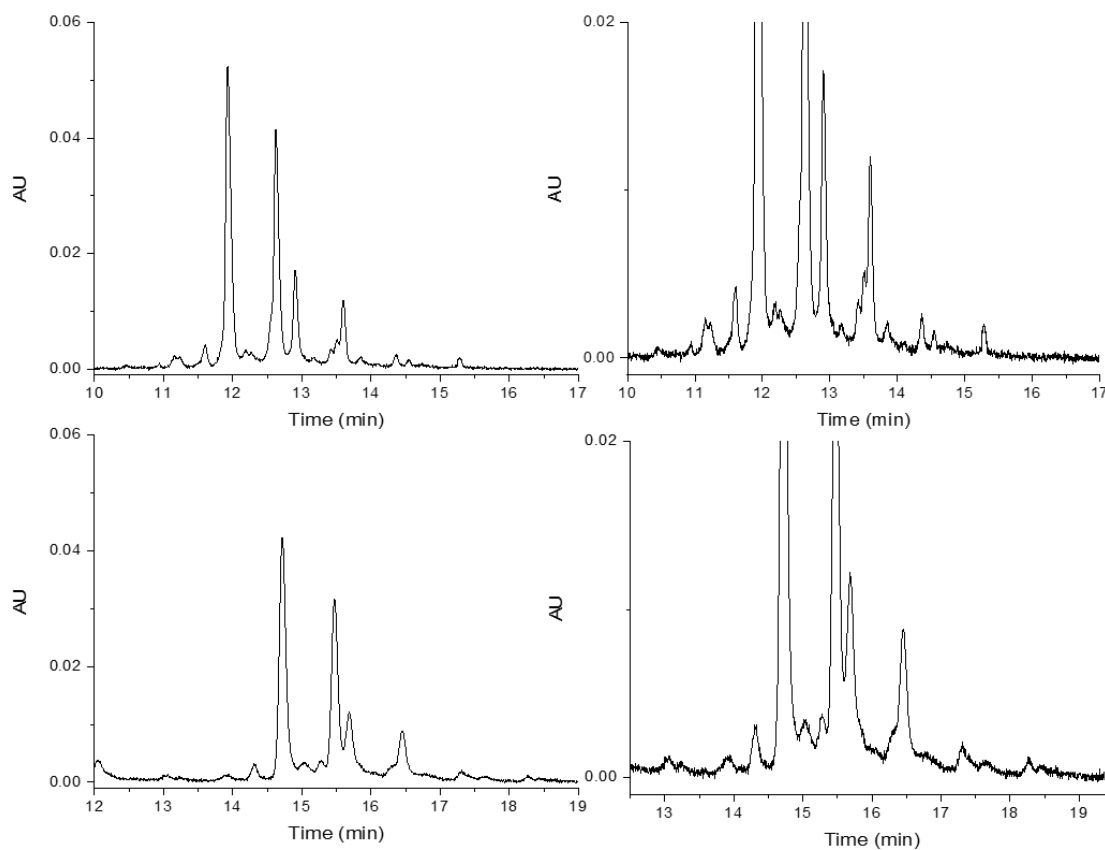Figure 5. 1 Ides and DTT work flow for glycoprotein analysis.

Figure 5. 2 NIST mAb comparrsion Copolymer (top) and Commercial column (botton). Temperature for the copolymer and commercial columns were 40 °C amd 60°C, respectivly. It can be seen that more glycoforms are seperated in the copolymer column than the commercial column.
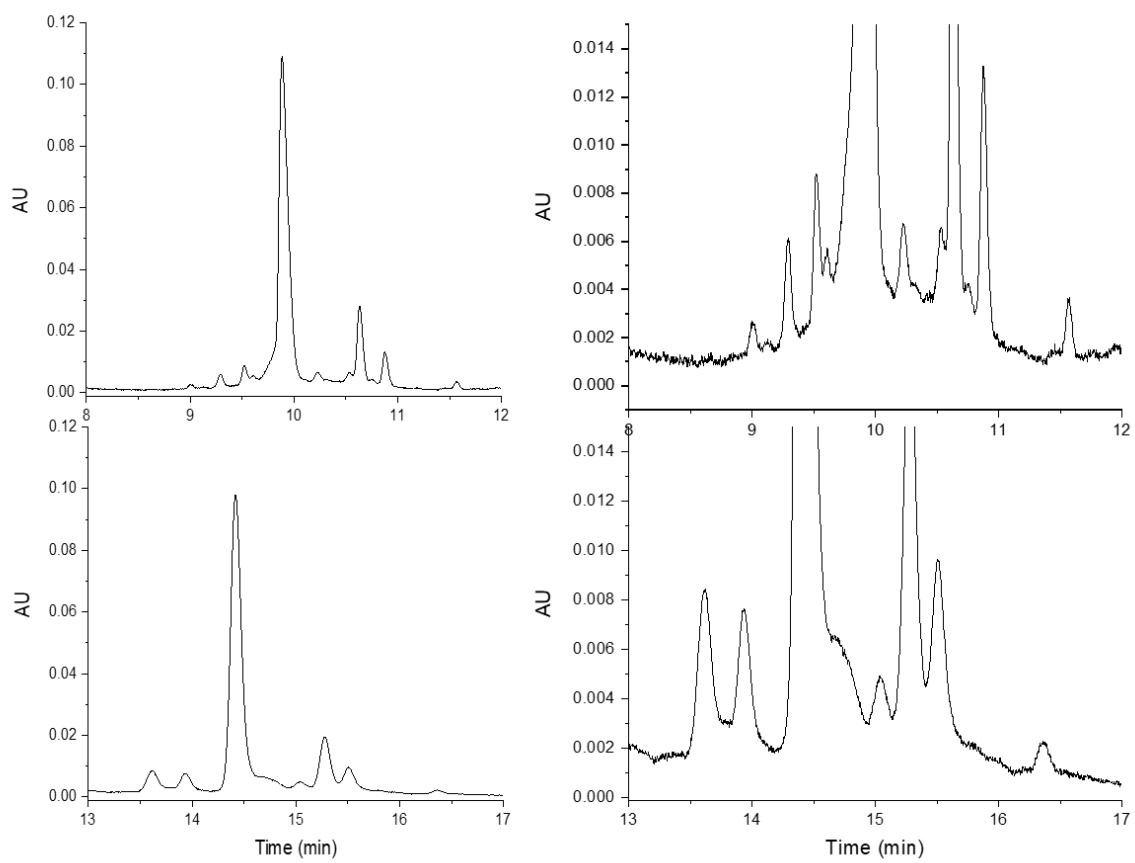
Figure 5. 3 Genentech comparison between copolymer (top) and commercial column (bottom). 50 °C and 70°C were used for the lab made and commercial column respectively. Higher resolution is achieved with the lab made column than the commercial column.
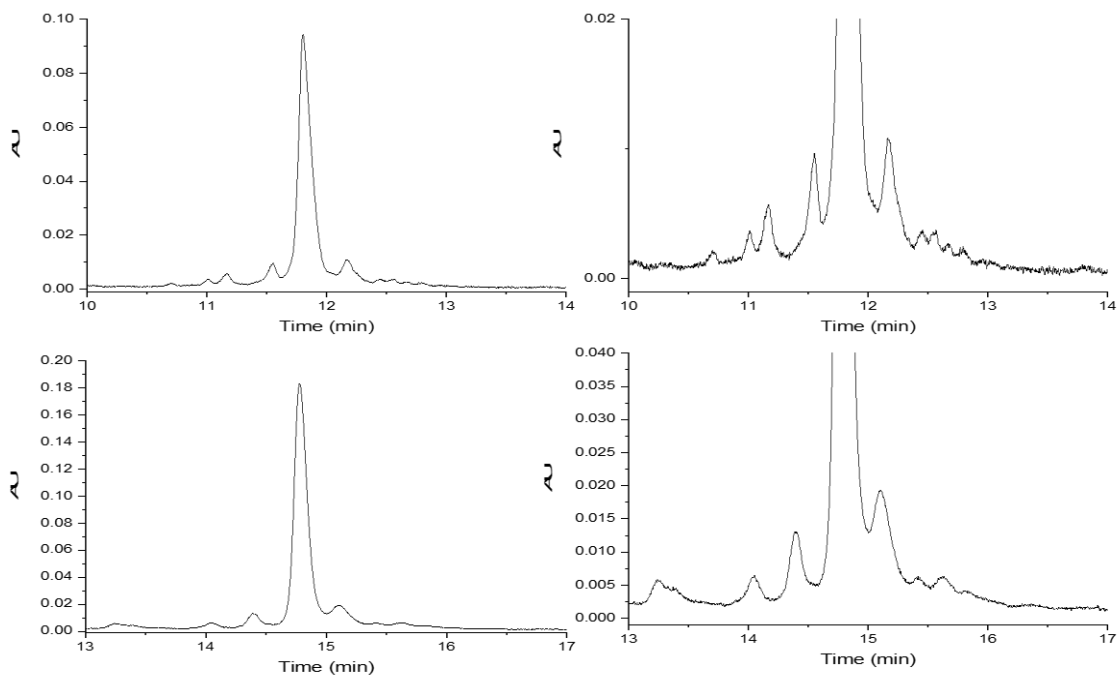
Figure 5. 4 AbbVie mAb IgG1 comparison between copolymer and commercial column. 50°C and 70°C was used for the lab made and commercial column respectively. More glycoforms are able to be separated in the lab made column than the commercial column..
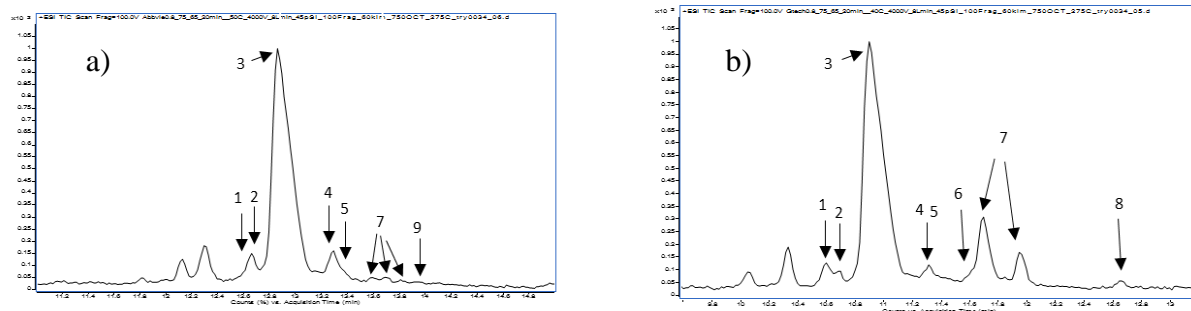
Figure 5. 5 Total Ion Chromatograms for (a) AbbVie IgG1 and (b) Genentech IgG1 lab made column separation. Peak assignments are as followed, 1-G0, 2-G0F-N, 3-G0F, 4-Man5, 5-G1, 6-G1F-N, 7- G1F, 8-G2F, 9-Man6

Label	Glycan	Mass	RT
1	Man3-F+N	24883.11	11.15
2	Man3+F	24826.78	11.23
3	G0	25086.96	11.5
4	Man3+F+N	25029.37	11.6
5	G0F	25232.61	11.93
6	man5	25004.10	12.19
7	G1	25248.69	12.28
8	G1F-N	25191.70	12.55
9	G1F	25394.68	12.63
10	G1F	25394.72	12.9
11	G1f+N	25598.00	13.4
12	G1f+N	25598.00	13.17
13	G2F	25556.51	13.42
14	G2F-N	25353.43	13.51
15	G1F-N+S	25498.54	13.53
16	G1f+N	25598.00	13.6
17	G1F+S	25701.72	13.6
18	G2F	25556.73	13.6
19	G1F+S	25701.72	14.1
20	G2F+N	25759.56	13.83
21	G2F	25556.52	13.85
22	G2F+G	25719.56	14.37
23	G2F+G	25718.64	14.54
24	Man5+N+G+G	25868.02	14.57
25	G3F	25920.84	14.72
26	G2F+2G	25880.94	15.29
27	G2F+SG	26024.73	15.29
28	G2FN+2G	26085.15	15.57

Figure 5. 6 Table of identified glycans through mass spectrometry of NIST mAb and corresponding retention time on LC chromatogram